Summary of ILD performance at SPS1a'

Mikael Berggren[1]

[1]DESY, Hamburg

Contribution to LCWS, Chicago, November 2008

Outline

Scope and people

What can be done if SUSY exists, and is "next to LEP", and we use a real detector ?

- Look at SPS1a'
- Run full simulation
- Study a ILD type detector

People involved

- Nicola d'Ascenzo
- Peter Schade
- Olga Stempel
- Supervisors: J. List, P. Bechtle, M.B.

The detector

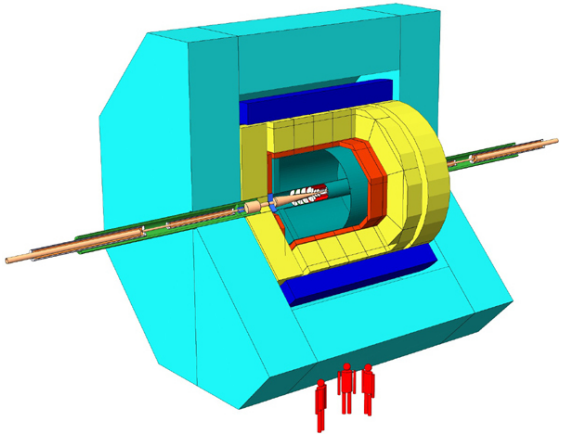

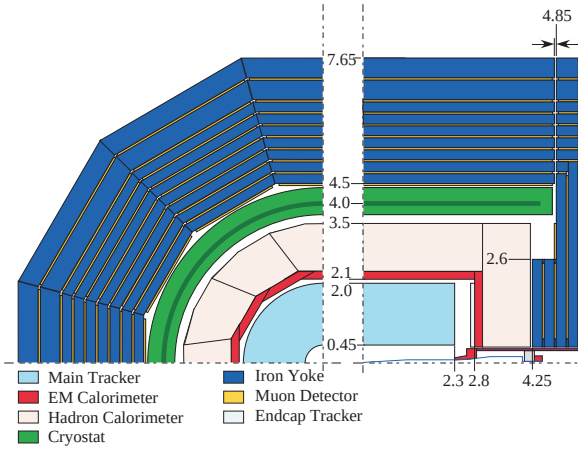

ILD: Merge the (mostly European) LDC and the (mostly Asiatic) GLD !

First meeting in January in Zeuthen.

Final merging decided in September in Cambridge.

Similar to the GLD' and the LDC' : Size and B-field intermediate to the original concepts, with LDC's calorimeters and GLD's vertex-detector.

The detector

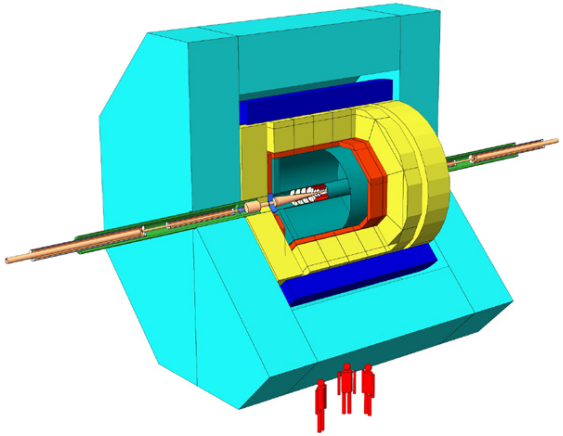

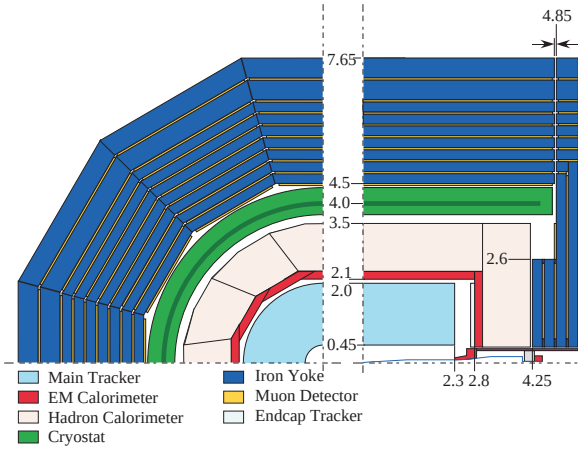

ILD: Merge the (mostly European) LDC and the (mostly Asiatic) GLD !

First meeting in January in Zeuthen.

Final merging decided in September in Cambridge.

Similar to the GLD' and the LDC' : Size and B-field intermediate to the original concepts, with LDC's calorimeters and GLD's vertex-detector.

The detector

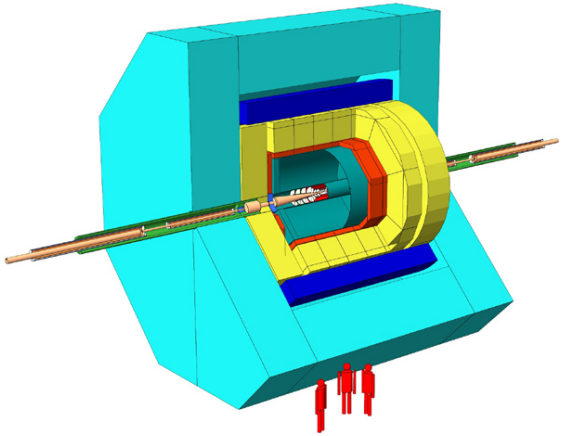

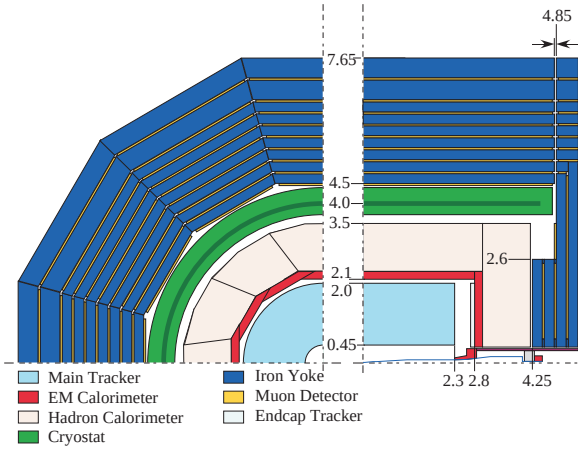

ILD: Merge the (mostly European) LDC and the (mostly Asiatic) GLD !

First meeting in January in Zeuthen.

Final merging decided in September in Cambridge.

Similar to the GLD' and the LDC' : Size and B-field intermediate to the original concepts, with LDC's calorimeters and GLD's vertex-detector.

The detector

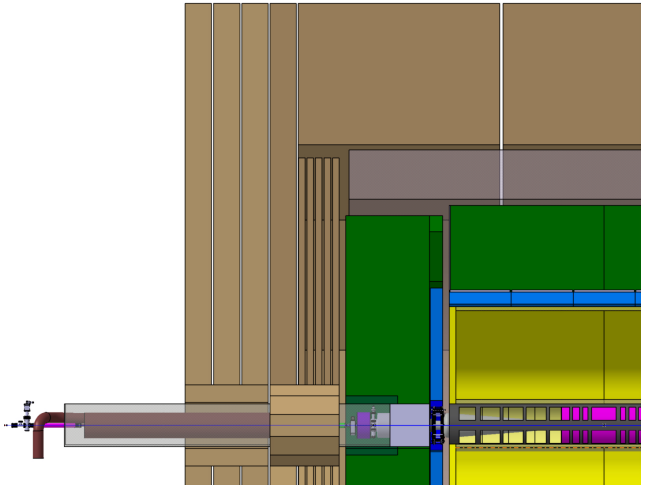

ILD: Merge the (mostly European) LDC and the (mostly Asiatic) GLD !

First meeting in January in Zeuthen.

Final merging decided in September in Cambridge.

Similar to the GLD' and the LDC' : Size and B-field intermediate to the original concepts, with LDC's calorimeters and GLD's vertex-detector.

The detector

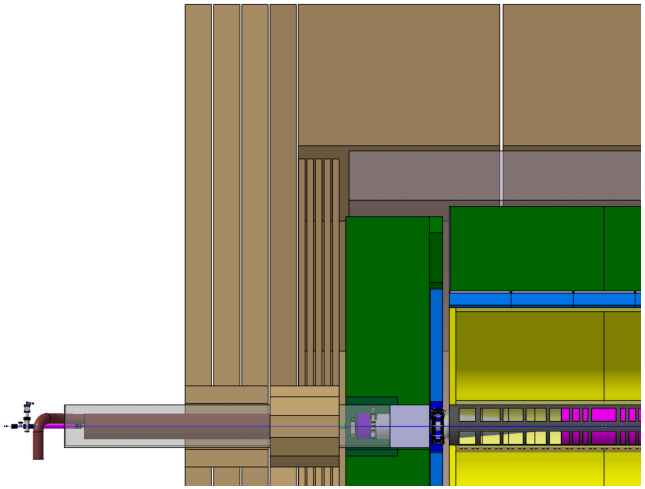

ILD: Merge the (mostly European) LDC and the (mostly Asiatic) GLD !

First meeting in January in Zeuthen.

Final merging decided in September in Cambridge.

Similar to the GLD' and the LDC' : Size and B-field intermediate to the original concepts, with LDC's calorimeters and GLD's vertex-detector.

Analyses presented here are based on full simulation of LDC'.

SPS1a'

Pure mSUGRA model:

$M_{1/2} = 250\mathrm{GeV}, M_0 = 70\mathrm{GeV}, A_0 = -300\mathrm{GeV}, \tan\beta = 10, sign(\mu) = +1$

Just outside what is excluded by LEP and low-energy observations. Compatible with WMAP, with $\tilde{\chi}_1^0$ Dark Matter.

- All sleptons available.
- No squarks.
- Lighter bosinos, up to $\tilde{\chi}_3^0$ (in $\mathrm{e}^+\mathrm{e}^- \rightarrow \tilde{\chi}_1^0\tilde{\chi}_3^0$)

Reported here: Final analysis of μ channels (Nicola d'Ascenzo)
Status report on $\tilde{\tau}_1$ channel (Peter Schade and Olga Stempel).

SPS1a'

Pure mSUGRA model:

$M_{1/2} = 250\mathrm{GeV}, M_0 = 70\mathrm{GeV}, A_0 = -300\mathrm{GeV}, \tan\beta = 10, sign(\mu) = +1$

Just outside what is excluded by LEP and low-energy observations. Compatible with WMAP, with $\tilde{\chi}_1^0$ Dark Matter.

- All sleptons available.
- No squarks.
- Lighter bosinos, up to $\tilde{\chi}_3^0$ (in $\mathrm{e}^+\mathrm{e}^- \rightarrow \tilde{\chi}_1^0\tilde{\chi}_3^0$)

Reported here: Final analysis of μ channels (Nicola d'Ascenzo)
Status report on $\tilde{\tau}_1$ channel (Peter Schade and Olga Stempel).

μ channels

Looking at the "right polarisation" (e^- left, e^+ right).

- $\tilde{\mu}_L\tilde{\mu}_L \rightarrow \mu\mu\tilde{\chi}_1^0\tilde{\chi}_1^0$
- $\tilde{\chi}_1^0\tilde{\chi}_2^0 \rightarrow \mu\tilde{\mu}_R\tilde{\chi}_1^0 \rightarrow \mu\mu\tilde{\chi}_1^0\tilde{\chi}_1^0$

- $\tilde{\mu}_L\tilde{\mu}_L$: Large cross-section. Find $M_{\tilde{\mu}_L}$ and $M_{\tilde{\chi}_1^0}$
- $\tilde{\chi}_1^0\tilde{\chi}_2^0$: Small cross-section X BR. Find $M_{\tilde{\chi}_2^0}$.

Backgrounds

- Each process is background to the other
- Other SUSY giving two μ:s. Mainly $\tilde{\mu}_R\tilde{\mu}_R$. Also $\tilde{\tau}\tilde{\tau}$ with $\tau \rightarrow \mu\nu_\mu\nu_\tau$
- SM, mainly WW and ZZ.

Kinematic variables

- Momentum of μ:s
- Acolinearity angle.
- Acoplanarity angle.
- Missing P_T.
- $M_{\mu\mu}$
- E_{miss}
- $\theta_{missing\ p}$
- β of μ system.

Kinematic variables

- Momentum of μ:s
- Acolinearity angle.
- Acoplanarity angle.
- Missing P_T.
- $M_{\mu\mu}$
- E_{miss}
- $\theta_{missing\ p}$
- β of μ system.

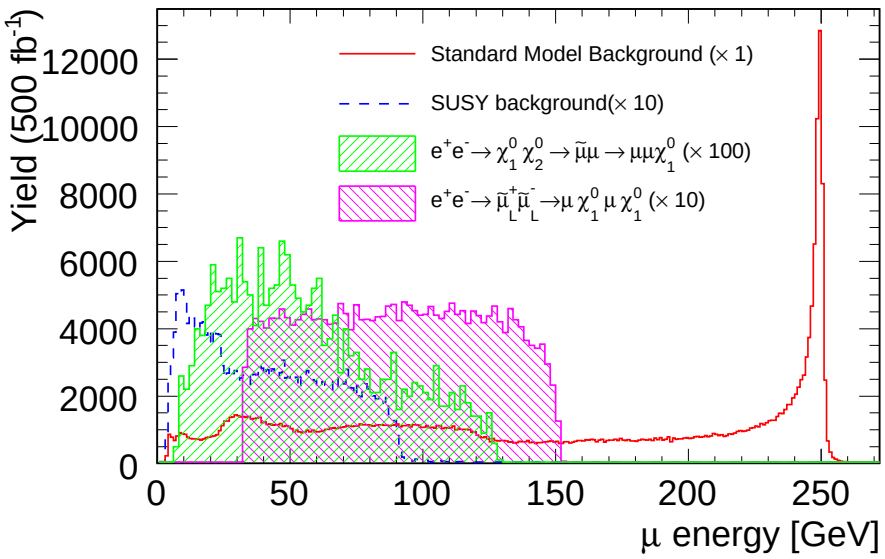

Kinematic variables

- Momentum of μ:s
- Acolinearity angle.
- Acoplanarity angle.
- Missing P_T.
- $M_{\mu\mu}$
- E_{miss}
- $\theta_{missing\ p}$
- β of μ system.

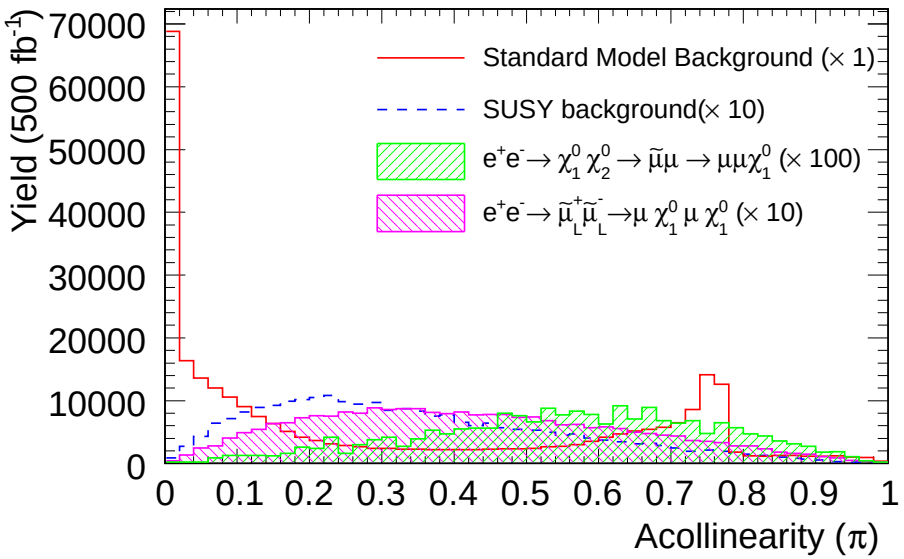

Kinematic variables

- Momentum of μ:s
- Acolinearity angle.
- Acoplanarity angle.
- Missing P_T.
- $M_{\mu\mu}$
- E_{miss}
- $\theta_{missing\ p}$
- β of μ system.

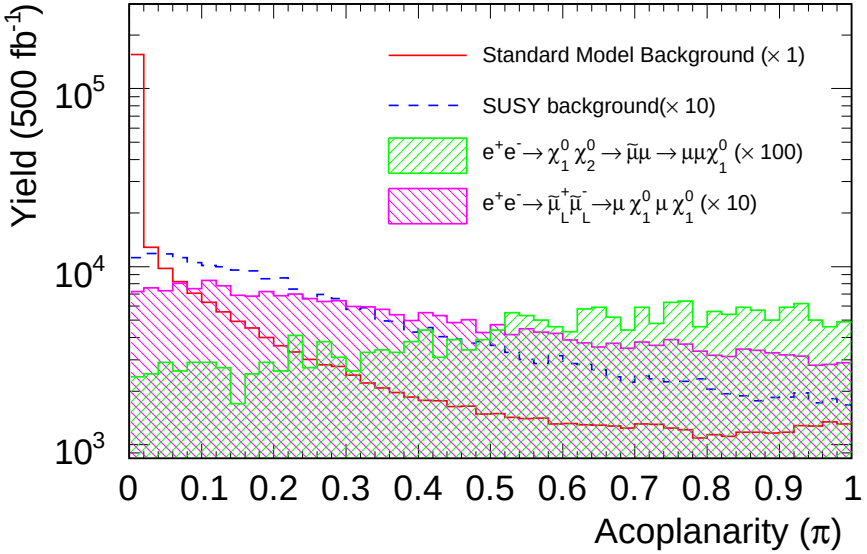

Kinematic variables

- Momentum of μ:s
- Acolinearity angle.
- Acoplanarity angle.
- Missing P_T.
- $M_{\mu\mu}$
- E_{miss}
- $\theta_{missing\ p}$
- β of μ system.

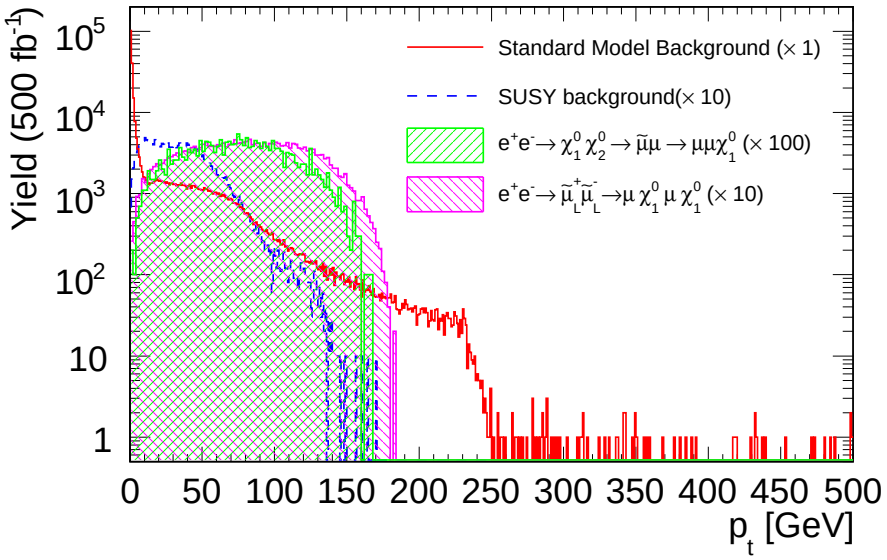

Kinematic variables

- Momentum of μ:s
- Acolinearity angle.
- Acoplanarity angle.
- Missing P_T.
- $M_{\mu\mu}$
- E_{miss}
- $\theta_{missing\ p}$
- β of μ system.

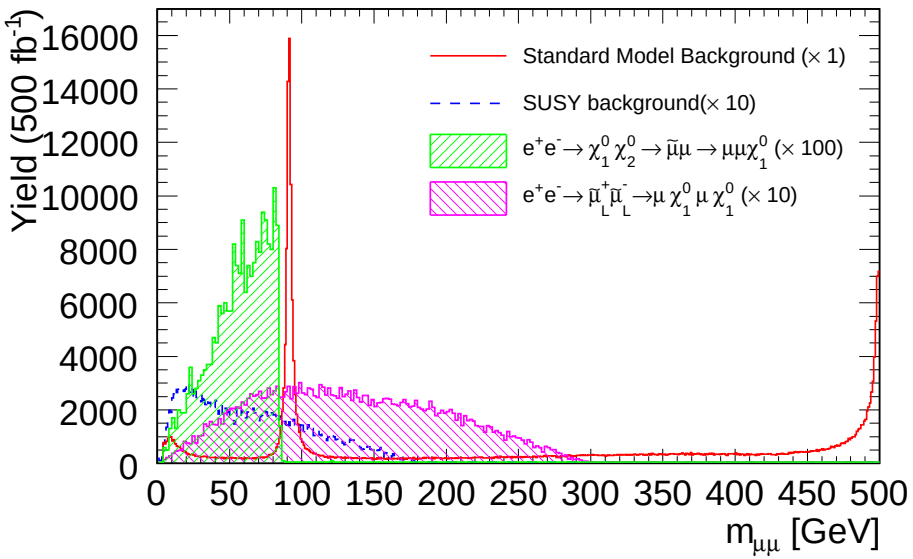

Kinematic variables

- Momentum of μ:s
- Acolinearity angle.
- Acoplanarity angle.
- Missing P_T.
- $M_{\mu\mu}$
- E_{miss}
- $\theta_{missing\ p}$
- β of μ system.

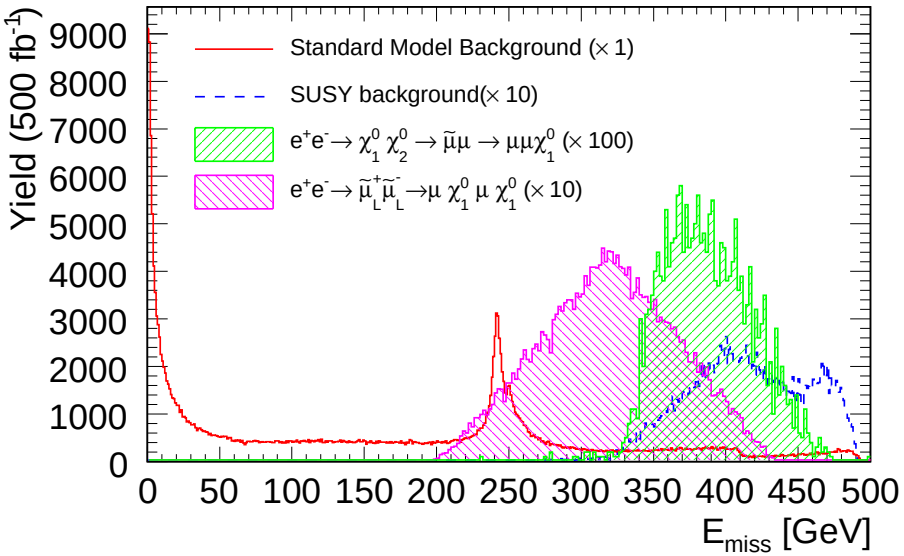

Kinematic variables

- Momentum of μ:s
- Acolinearity angle.
- Acoplanarity angle.
- Missing P_T.
- $M_{\mu\mu}$
- E_{miss}
- $\theta_{missing\ p}$
- β of μ system.

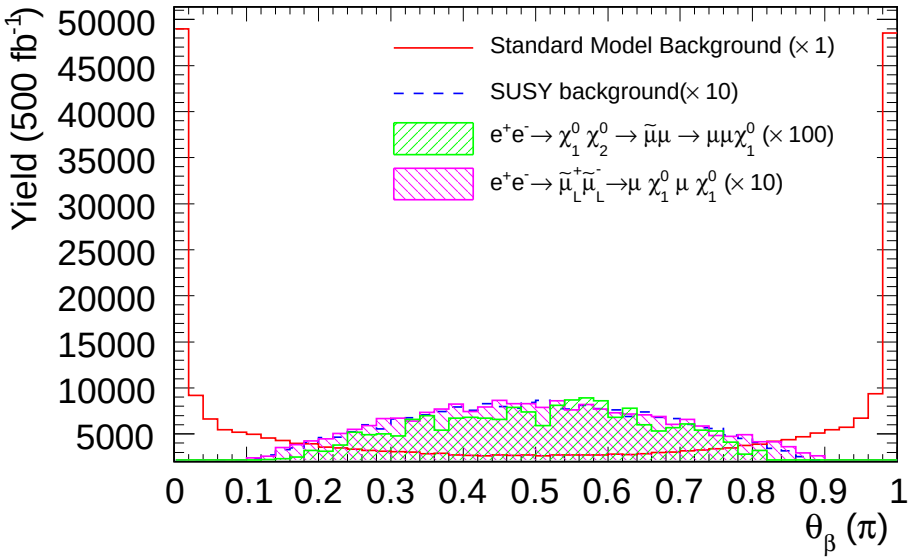

Kinematic variables

- Momentum of μ:s
- Acolinearity angle.
- Acoplanarity angle.
- Missing P_T.
- $M_{\mu\mu}$
- E_{miss}
- $\theta_{missing\ p}$
- β of μ system.

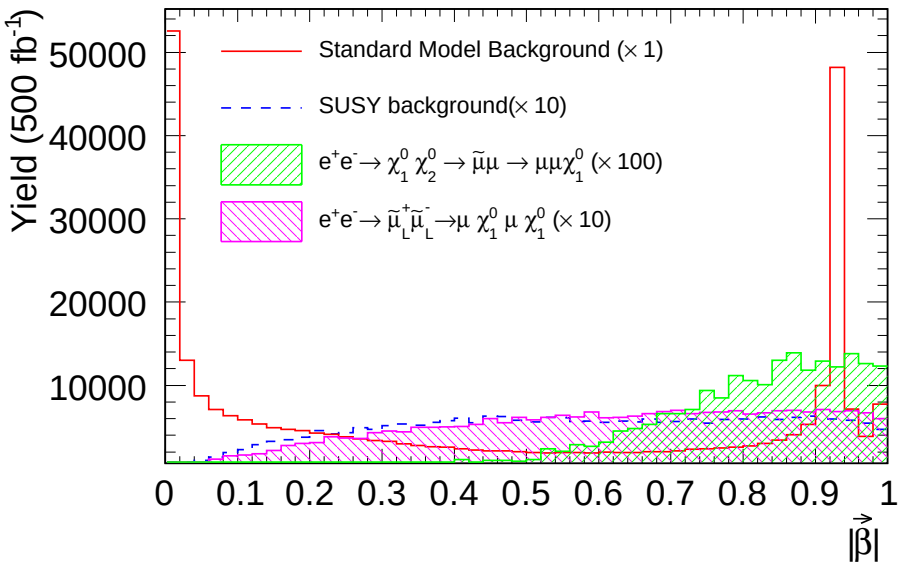

$\tilde{\mu}_L\tilde{\mu}_L$

Selections

- $E_{miss} \in [200, 430]\mathrm{GeV}$
- $M_{\mu\mu} \notin [80, 100]\mathrm{GeV}$ and $< 30\mathrm{GeV}/c^2$
- $\theta_{missing\ p} \in [0.1\pi, 0.9\pi]$

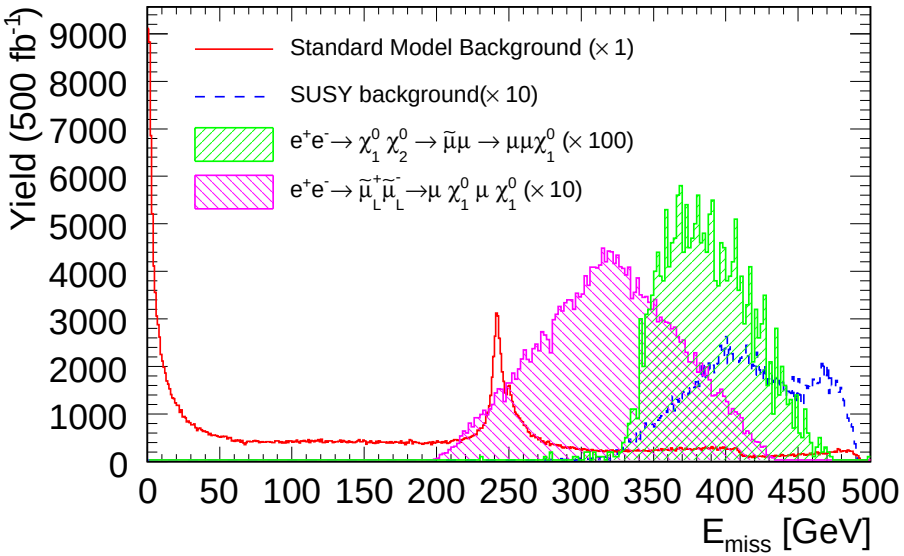

$\tilde{\mu}_L\tilde{\mu}_L$

Selections

- $E_{miss} \in [200, 430]\mathrm{GeV}$
- $M_{\mu\mu} \notin [80, 100]\mathrm{GeV}$ and $< 30\mathrm{GeV}/c^2$
- $\theta_{missing\ p} \in [0.1\pi, 0.9\pi]$

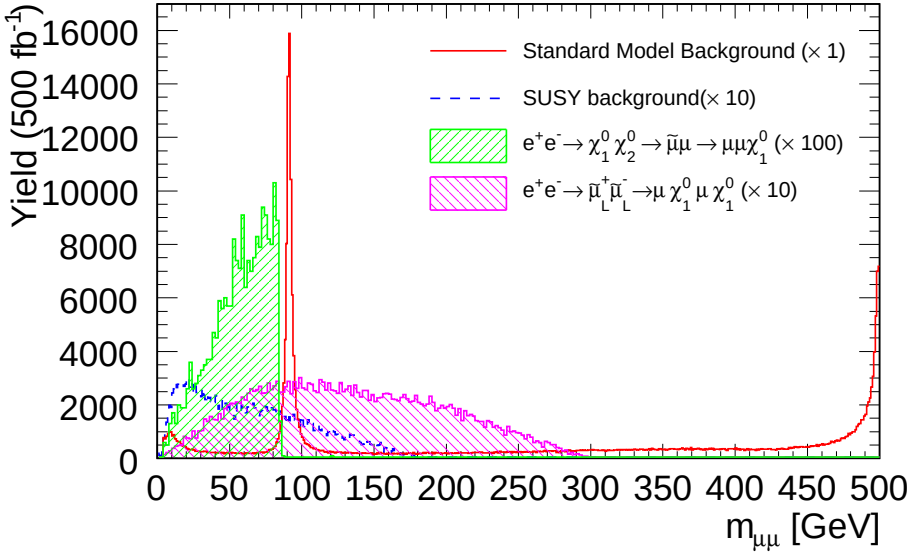

$\tilde{\mu}_L\tilde{\mu}_L$

Selections

- $E_{miss} \in [200, 430]\mathrm{GeV}$
- $M_{\mu\mu} \notin [80, 100]\mathrm{GeV}$ and $< 30\mathrm{GeV}/c^2$
- $\theta_{missing\ p} \in [0.1\pi, 0.9\pi]$

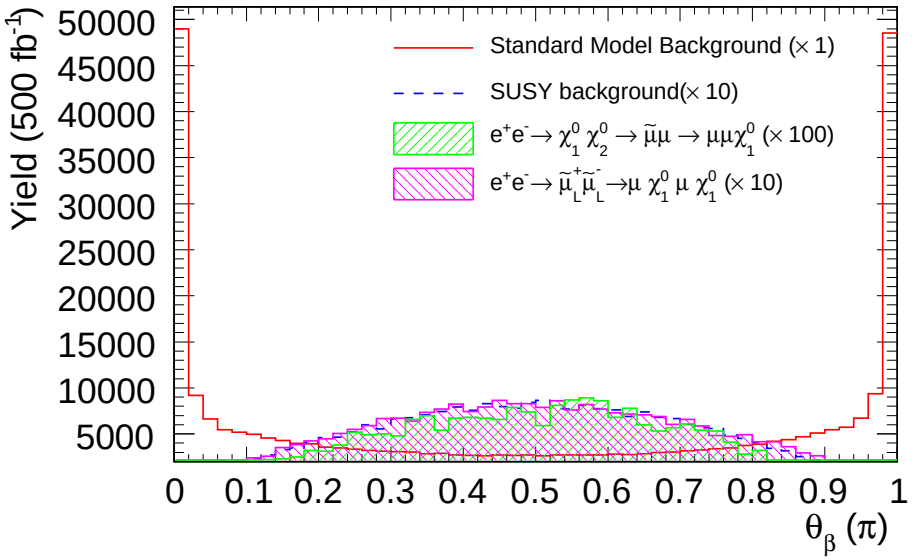

$\tilde{\mu}_L\tilde{\mu}_L$

Selections

- $E_{miss} \in [200, 430]\mathrm{GeV}$
- $M_{\mu\mu} \notin [80, 100]\mathrm{GeV}$ and $< 30\mathrm{GeV}/c^2$
- $\theta_{missing\ p} \in [0.1\pi, 0.9\pi]$

Masses from edges. Beam-energy spread dominates error.

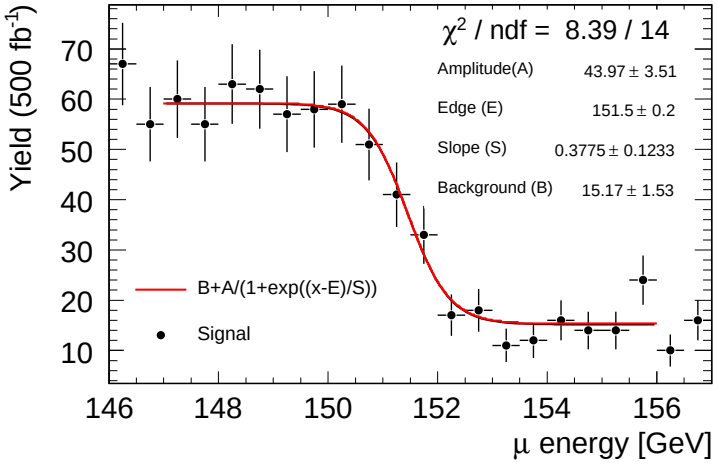

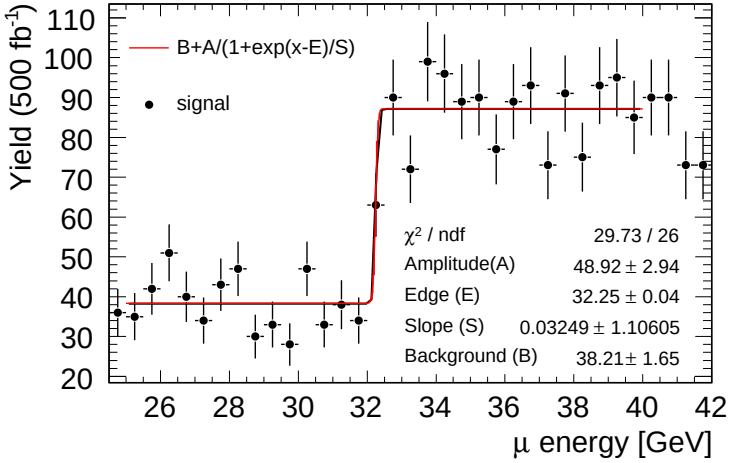

$\tilde{\mu}_L\tilde{\mu}_L$

Selections

- $E_{miss} \in [200, 430]\mathrm{GeV}$
- $M_{\mu\mu} \notin [80, 100]\mathrm{GeV}$ and $< 30\mathrm{GeV}/c^2$
- $\theta_{missing\ p} \in [0.1\pi, 0.9\pi]$

Masses from edges. Beam-energy spread dominates error.
Cross-section from extended likelihood ($L(p_{T\mu}, \theta_{acol})$)

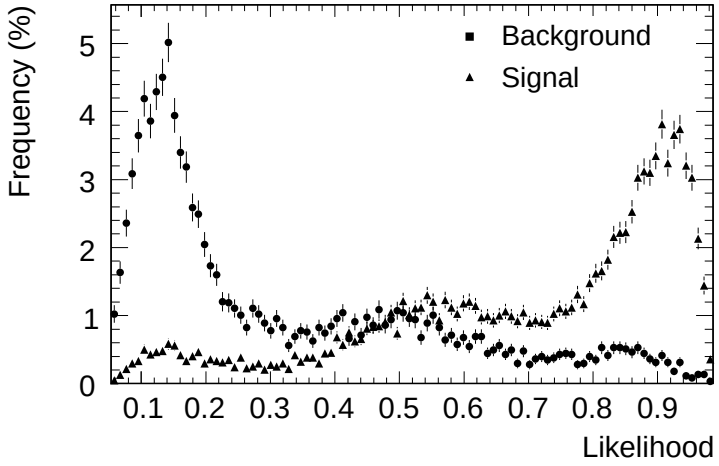

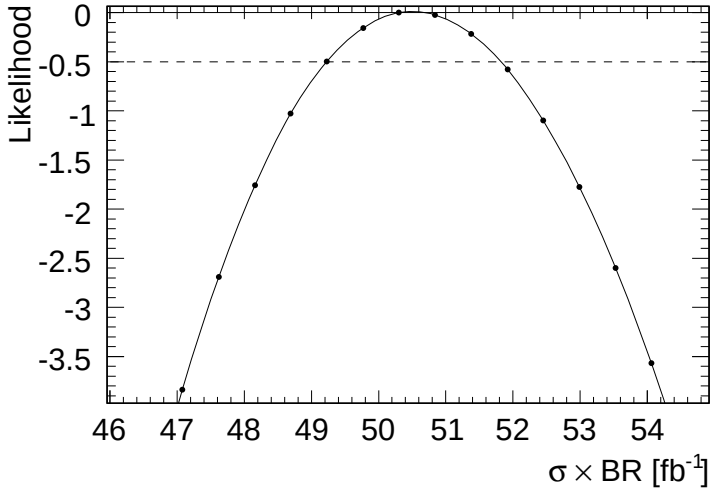

$\tilde{\mu}_L\tilde{\mu}_L$

Selections

- $E_{miss} \in [200, 430]\mathrm{GeV}$
- $M_{\mu\mu} \notin [80, 100]\mathrm{GeV}$ and $< 30\mathrm{GeV}/c^2$
- $\theta_{missing\ p} \in [0.1\pi, 0.9\pi]$

Masses from edges. Beam-energy spread dominates error.
Cross-section from extended likelihood ($L(p_{T\mu}, \theta_{acol})$)

$\Delta(M_{\tilde{\chi}_1^0}) = 920\mathrm{MeV}/c^2$
$\Delta(M_{\tilde{\mu}_L}) = 100\mathrm{MeV}/c^2$
$\Delta(\sigma(\mathrm{e}^+\mathrm{e}^- \rightarrow \tilde{\mu}_L\tilde{\mu}_L))$ = 1.35 fb.

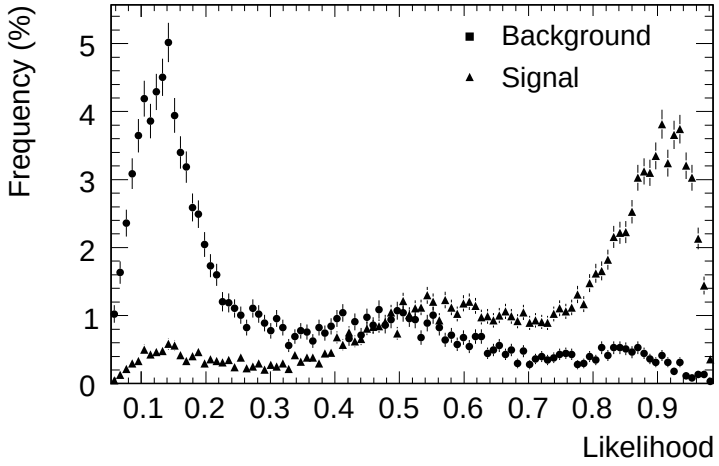

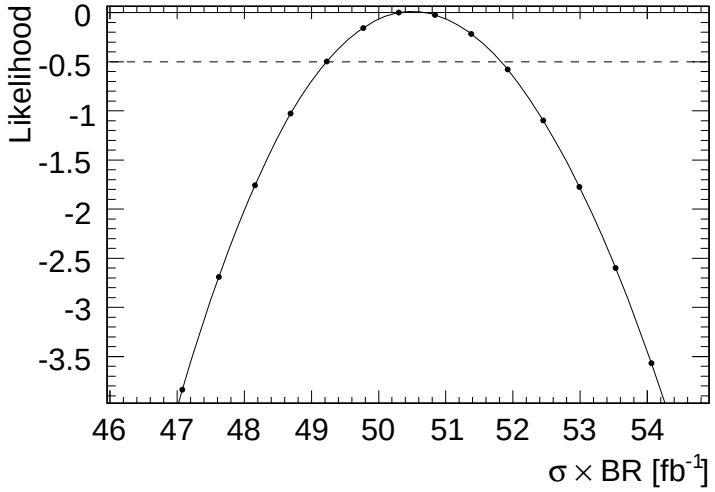

$\tilde{\chi}_1^0\tilde{\chi}_2^0$

Selections

- $\theta_{missing\ p} \in [0.2\pi, 0.8\pi]$
- β of μ system > 0.6.
- $E_{miss} \in [355, 395]\mathrm{GeV}/c^2$
- $p_{Tmiss} > 40\mathrm{GeV}/c$

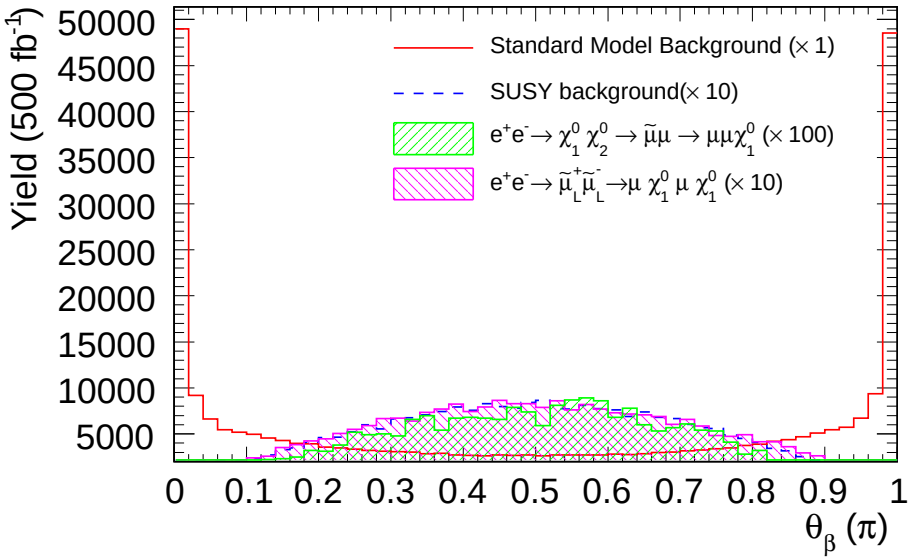

$\tilde{\chi}_1^0\tilde{\chi}_2^0$

Selections

- $\theta_{missing\ p} \in [0.2\pi, 0.8\pi]$
- β of μ system > 0.6.
- $E_{miss} \in [355, 395]\mathrm{GeV}/c^2$
- $p_{Tmiss} > 40\mathrm{GeV}/c$

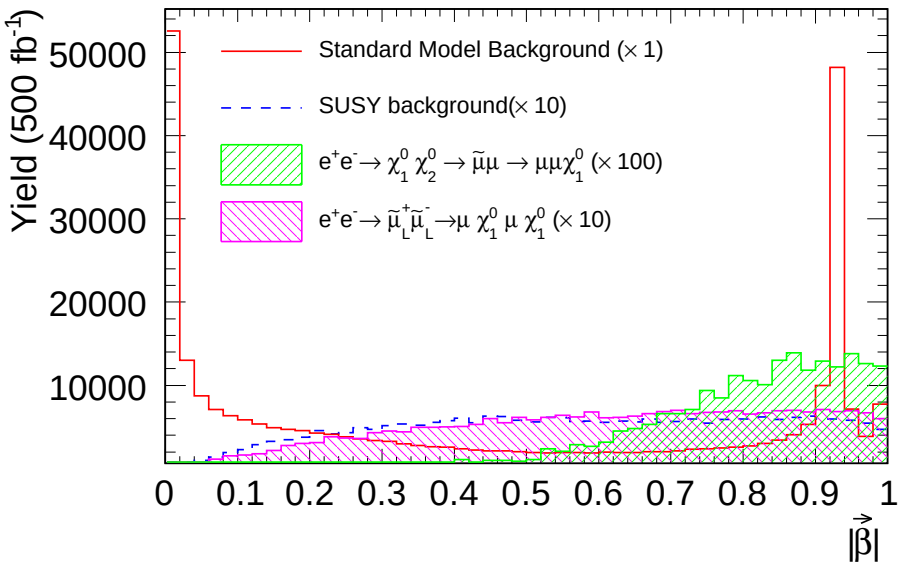

$\tilde{\chi}_1^0\tilde{\chi}_2^0$

Selections

- $\theta_{missing\ p} \in [0.2\pi, 0.8\pi]$
- β of μ system > 0.6.
- $E_{miss} \in [355, 395]\mathrm{GeV}/c^2$
- $p_{Tmiss} > 40\mathrm{GeV}/c$

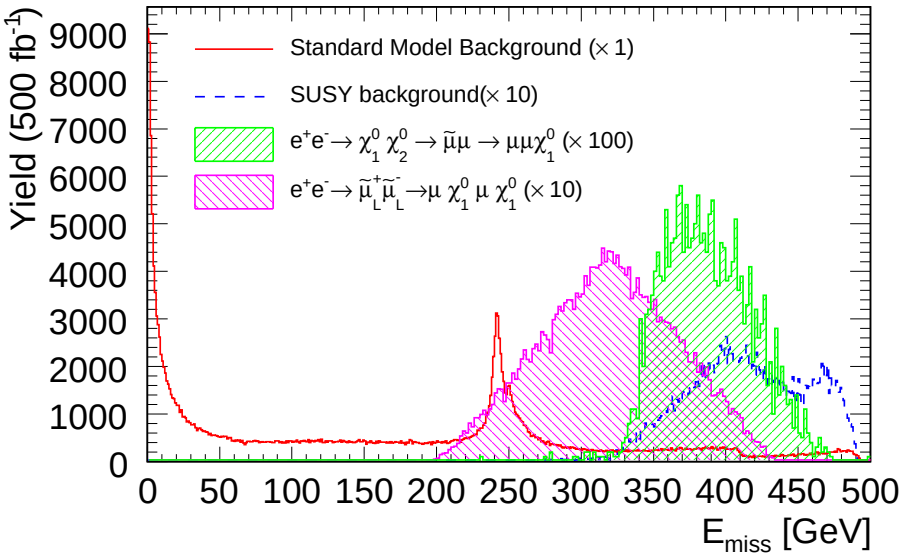

$\tilde{\chi}_1^0\tilde{\chi}_2^0$

Selections

- $\theta_{missing\ p} \in [0.2\pi, 0.8\pi]$
- β of μ system > 0.6.
- $E_{miss} \in [355, 395]\mathrm{GeV}/c^2$
- $p_{Tmiss} > 40\mathrm{GeV}/c$

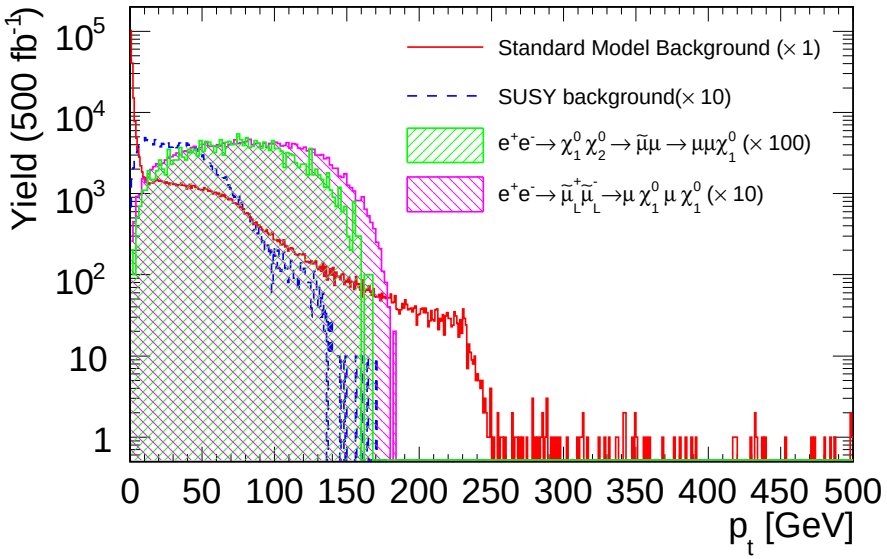

$\tilde{\chi}_1^0\tilde{\chi}_2^0$

Selections

- $\theta_{missing\ p} \in [0.2\pi, 0.8\pi]$
- β of μ system > 0.6.
- $E_{miss} \in [355, 395]\mathrm{GeV}/c^2$
- $p_{Tmiss} > 40\mathrm{GeV}/c$

Mass from fit to invariant mass edge.

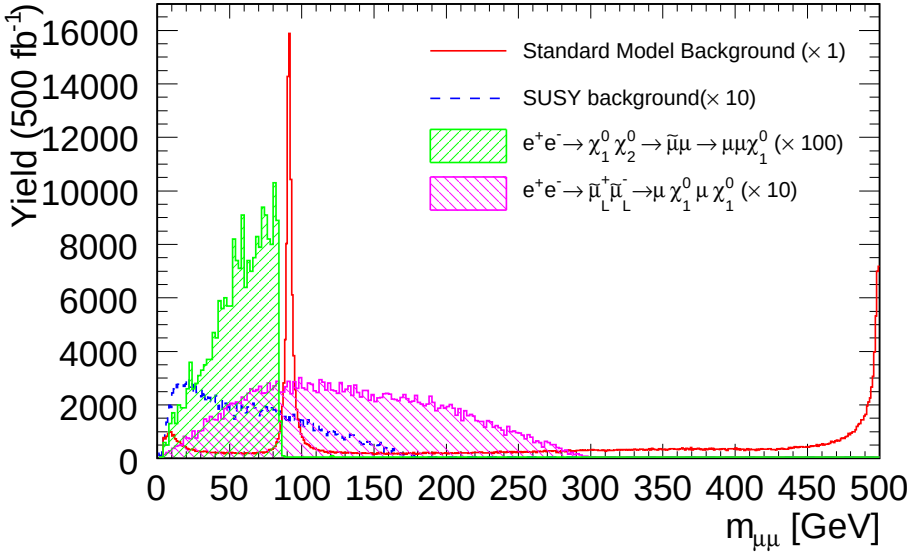

$\tilde{\chi}_1^0\tilde{\chi}_2^0$

Selections

- $\theta_{missing\ p} \in [0.2\pi, 0.8\pi]$
- β of μ system > 0.6.
- $E_{miss} \in [355, 395]\mathrm{GeV}/c^2$
- $p_{Tmiss} > 40\mathrm{GeV}/c$

Mass from fit to invariant mass edge.

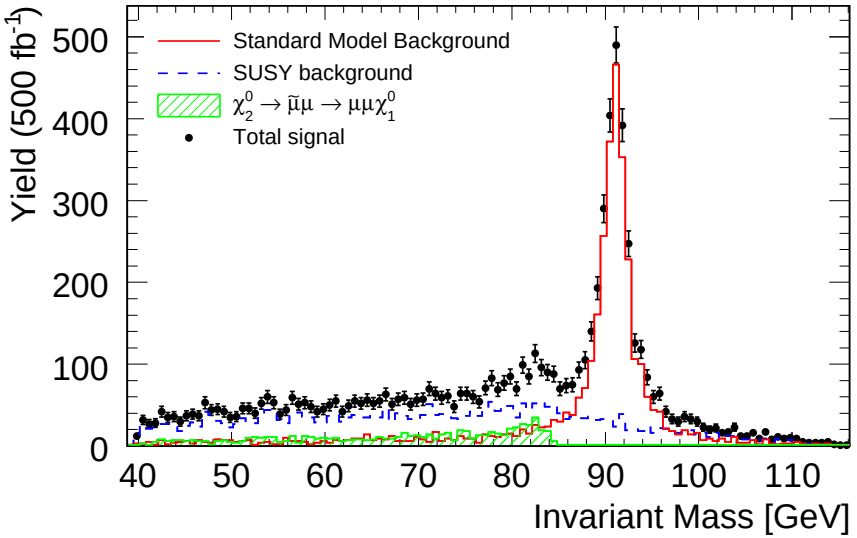

$\tilde{\chi}_1^0\tilde{\chi}_2^0$

Selections

- $\theta_{missing\ p} \in [0.2\pi, 0.8\pi]$
- β of μ system > 0.6.
- $E_{miss} \in [355, 395]\mathrm{GeV}/c^2$
- $p_{Tmiss} > 40\mathrm{GeV}/c$

Mass from fit to invariant mass edge.

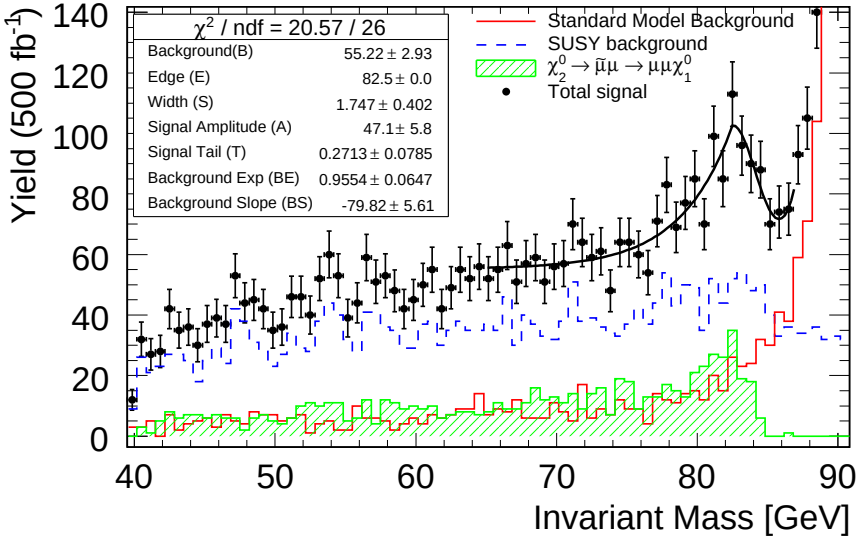

$\tilde{\chi}_1^0\tilde{\chi}_2^0$

Selections

- $\theta_{missing\ p} \in [0.2\pi, 0.8\pi]$
- β of μ system > 0.6.
- $E_{miss} \in [355, 395]\mathrm{GeV}/c^2$
- $p_{Tmiss} > 40\mathrm{GeV}/c$

Mass from fit to invariant mass edge.

$$\Delta(M_{\tilde{\chi}_2^0}) = 1.38\mathrm{GeV}/c^2$$

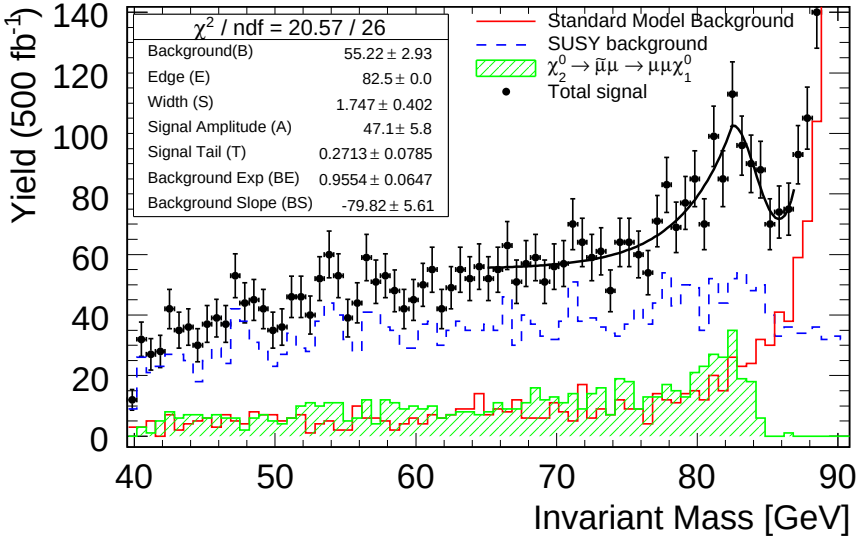

Status report on $\tilde{\tau}$:s

Issues and features:

- In SPS1a', the $\tilde{\tau}$ is the NLSP.
  $M_{\tilde{\tau}_1} = 107.9\mathrm{GeV}/c^2$, $M_{\tilde{\chi}_1^0} = 97.7\mathrm{GeV}/c^2$, so $\Delta(M) = 10.2\mathrm{GeV}/c^2$.
- $P_{\tilde{\tau},min} = 2.2\mathrm{GeV}/c$, $P_{\tilde{\tau},max} = 42.8\mathrm{GeV}/c$: $\gamma\gamma$ background, but is not included yet.
- Plays an important role for DM: $M_{\tilde{\tau}_1}$ important.
- The $\tilde{\tau}$ mass-eigenstates are expected to be different from the chiral ones. Off-diagonal terms of mass-matrix:
  $-M_\tau(A_{\tilde{\tau}} - \mu \tan\beta)$.
- Relates to the $\tilde{\tau}$ mixing: With $M_{\tilde{\mu}_\mathrm{L}}$ and $M_{\tilde{\mu}_\mathrm{R}}$, a measurement of θ_{mix} gives $A_{\tilde{\tau}} - \mu \tan\beta$.
- Cross-section and τ polarisation depends (differently) on θ_{mix}.
- If $\tilde{\chi}_1^0$ is purely bino - it is in SPS1a' - P_τ depends only on θ_{mix}.

Extracting the $\tilde{\tau}$ properties

- The mass from end-point and turn-over of spectrum = $P_{\tilde{\tau},min}$ and $P_{\tilde{\tau},max}$
- P from spectrum for exclusive decay-mode(s). Here: $\tau \rightarrow \pi^{+-}\nu_\tau$
- Extract the signal.
  - $E_{jet} < 50\mathrm{GeV}$. 97 %.
  - $M_{jet} < 2\mathrm{GeV}/c^2$. 84 %.
  - θ_{jet} above 20 degrees. 80 %.
  - Acoplanarity < 160 degrees. 53 %.
  - $P_T < 30\mathrm{GeV}/c$. 53 %.
  - $\cos\theta_{p(miss)} < 0.98$. 52 %.
  - P_T wrt. Thrust axis in $R\phi$ projection. 52 %.

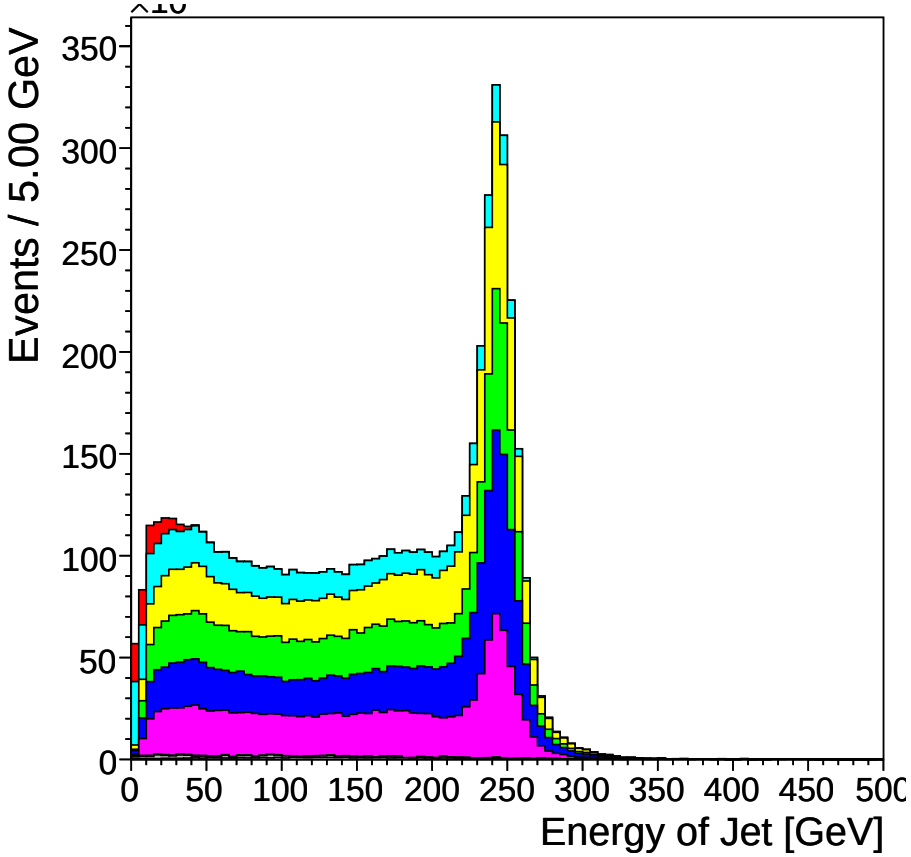

Extracting the $\tilde{\tau}$ properties

- The mass from end-point and turn-over of spectrum = $P_{\tilde{\tau},min}$ and $P_{\tilde{\tau},max}$
- P from spectrum for exclusive decay-mode(s). Here: $\tau \rightarrow \pi^{+-}\nu_\tau$
- Extract the signal.
  - $E_{jet} < 50\mathrm{GeV}$. 97 %.
  - $M_{jet} < 2\mathrm{GeV}/c^2$. 84 %.
  - θ_{jet} above 20 degrees. 80 %.
  - Acoplanarity < 160 degrees. 53 %.
  - $P_T < 30\mathrm{GeV}/c$. 53 %.
  - $\cos\theta_{p(miss)} < 0.98$. 52 %.
  - P_T wrt. Thrust axis in $R\phi$ projection. 52 %.

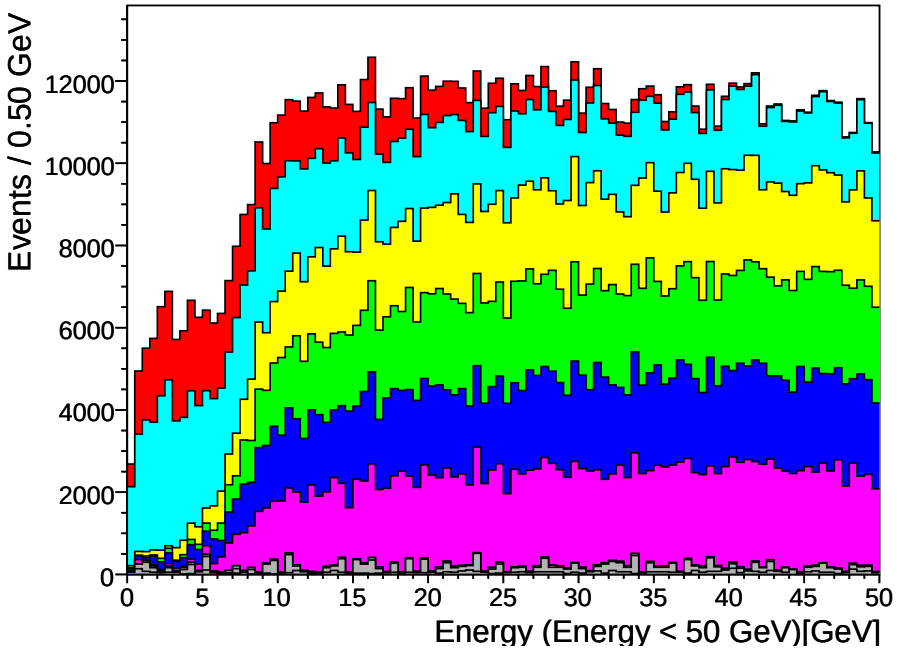

Extracting the $\tilde{\tau}$ properties

- The mass from end-point and turn-over of spectrum = $P_{\tilde{\tau},min}$ and $P_{\tilde{\tau},max}$
- P from spectrum for exclusive decay-mode(s). Here: $\tau \rightarrow \pi^{+-}\nu_\tau$
- Extract the signal.
  - $E_{jet} < 50\mathrm{GeV}$. 97 %.
  - $M_{jet} < 2\mathrm{GeV}/c^2$. 84 %.
  - θ_{jet} above 20 degrees. 80 %.
  - Acoplanarity < 160 degrees. 53 %.
  - $P_T < 30\mathrm{GeV}/c$. 53 %.
  - $\cos\theta_{p(miss)} < 0.98$. 52 %.
  - P_T wrt. Thrust axis in $R\phi$ projection. 52 %.

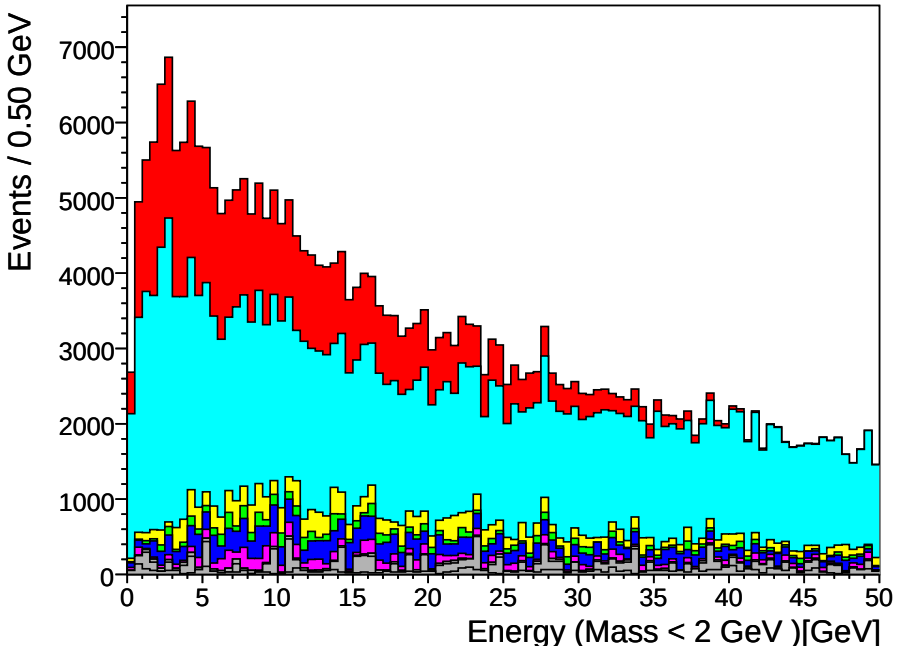

Extracting the $\tilde{\tau}$ properties

- The mass from end-point and turn-over of spectrum = $P_{\tilde{\tau},min}$ and $P_{\tilde{\tau},max}$
- P from spectrum for exclusive decay-mode(s). Here: $\tau \rightarrow \pi^{+-}\nu_\tau$
- Extract the signal.
  - $E_{jet} < 50\mathrm{GeV}$. 97 %.
  - $M_{jet} < 2\mathrm{GeV}/c^2$. 84 %.
  - θ_{jet} above 20 degrees. 80 %.
  - Acoplanarity < 160 degrees. 53 %.
  - $P_T < 30\mathrm{GeV}/c$. 53 %.
  - $\cos\theta_{p(miss)} < 0.98$. 52 %.
  - P_T wrt. Thrust axis in $R\phi$ projection. 52 %.

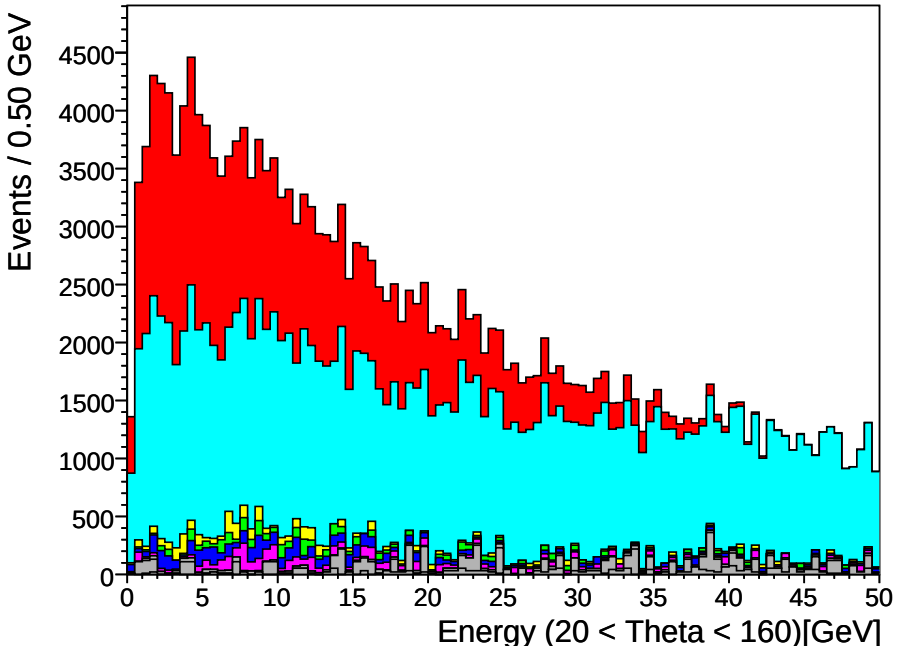

Extracting the $\tilde{\tau}$ properties

- The mass from end-point and turn-over of spectrum = $P_{\tilde{\tau},min}$ and $P_{\tilde{\tau},max}$
- P from spectrum for exclusive decay-mode(s). Here: $\tau \rightarrow \pi^{+-}\nu_\tau$
- Extract the signal.
  - $E_{jet} < 50\mathrm{GeV}$. 97 %.
  - $M_{jet} < 2\mathrm{GeV}/c^2$. 84 %.
  - θ_{jet} above 20 degrees. 80 %.
  - Acoplanarity < 160 degrees. 53 %.
  - $P_T < 30\mathrm{GeV}/c$. 53 %.
  - $\cos\theta_{p(miss)} < 0.98$. 52 %.
  - P_T wrt. Thrust axis in $R\phi$ projection. 52 %.

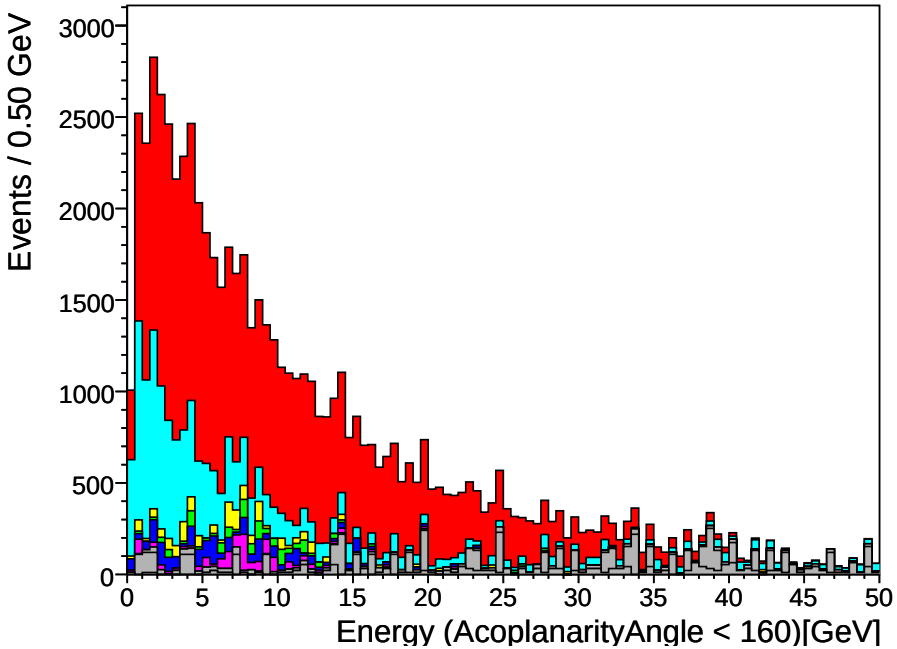

Extracting the $\tilde{\tau}$ properties

- The mass from end-point and turn-over of spectrum = $P_{\tilde{\tau},min}$ and $P_{\tilde{\tau},max}$
- P from spectrum for exclusive decay-mode(s). Here: $\tau \rightarrow \pi^{+-}\nu_\tau$
- Extract the signal.
  - $E_{jet} < 50\mathrm{GeV}$. 97 %.
  - $M_{jet} < 2\mathrm{GeV}/c^2$. 84 %.
  - θ_{jet} above 20 degrees. 80 %.
  - Acoplanarity < 160 degrees. 53 %.
  - $P_T < 30\mathrm{GeV}/c$. 53 %.
  - $\cos\theta_{p(miss)} < 0.98$. 52 %.
  - P_T wrt. Thrust axis in $R\phi$ projection. 52 %.

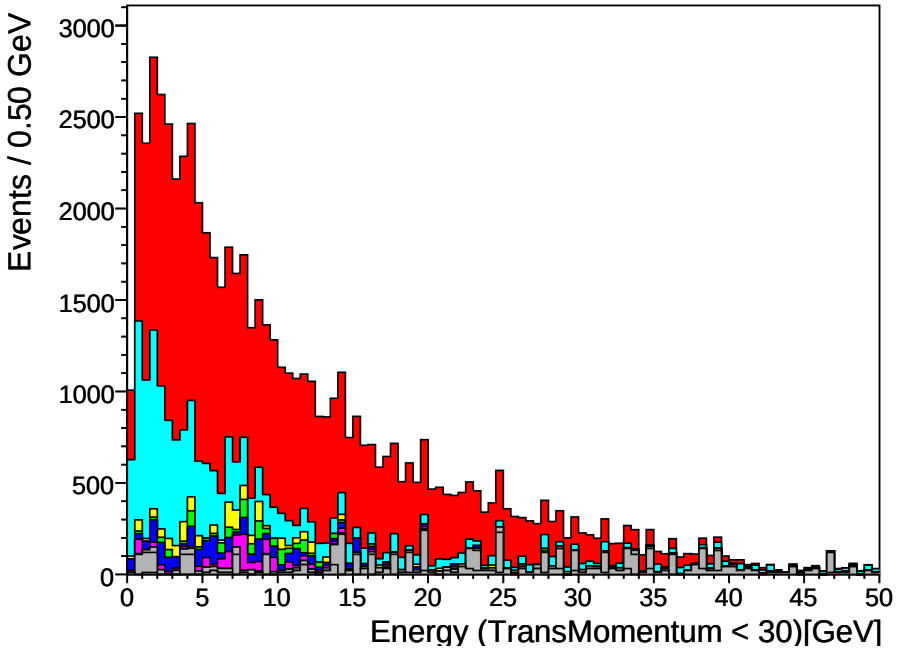

Extracting the $\tilde{\tau}$ properties

- The mass from end-point and turn-over of spectrum = $P_{\tilde{\tau},min}$ and $P_{\tilde{\tau},max}$
- P from spectrum for exclusive decay-mode(s). Here: $\tau \rightarrow \pi^{+-}\nu_\tau$
- Extract the signal.
  - $E_{jet} < 50\mathrm{GeV}$. 97 %.
  - $M_{jet} < 2\mathrm{GeV}/c^2$. 84 %.
  - θ_{jet} above 20 degrees. 80 %.
  - Acoplanarity < 160 degrees. 53 %.
  - $P_T < 30\mathrm{GeV}/c$. 53 %.
  - $\cos\theta_{p(miss)} < 0.98$. 52 %.
  - P_T wrt. Thrust axis in $R\phi$ projection. 52 %.

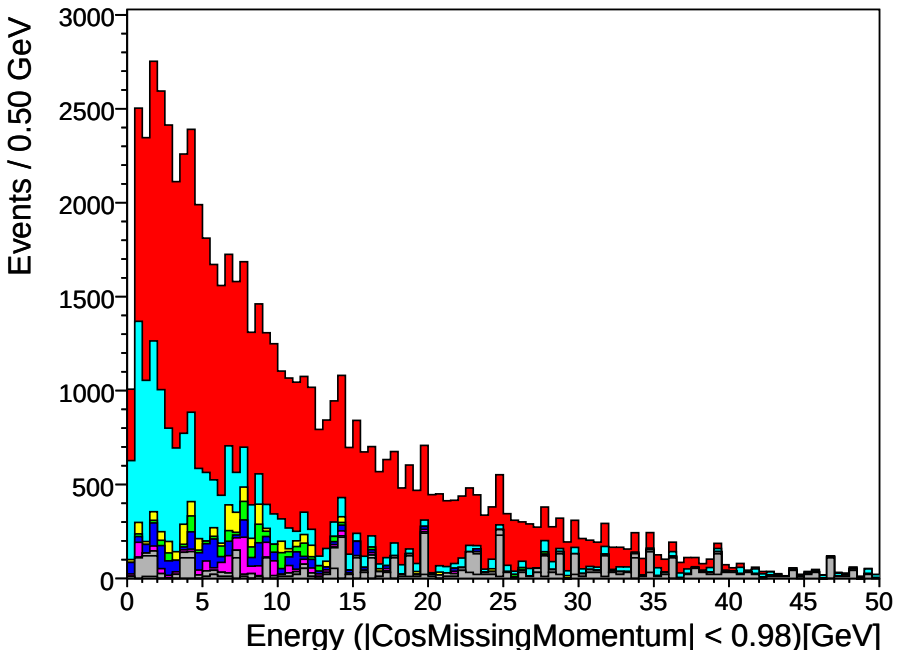

Extracting the $\tilde{\tau}$ properties

- The mass from end-point and turn-over of spectrum = $P_{\tilde{\tau},min}$ and $P_{\tilde{\tau},max}$
- P from spectrum for exclusive decay-mode(s). Here: $\tau \rightarrow \pi^{+-}\nu_\tau$
- Extract the signal.
  - $E_{jet} < 50\mathrm{GeV}$. 97 %.
  - $M_{jet} < 2\mathrm{GeV}/c^2$. 84 %.
  - θ_{jet} above 20 degrees. 80 %.
  - Acoplanarity < 160 degrees. 53 %.
  - $P_T < 30\mathrm{GeV}/c$. 53 %.
  - $\cos\theta_{p(miss)} < 0.98$. 52 %.
  - P_T wrt. Thrust axis in $R\phi$ projection. 52 %.

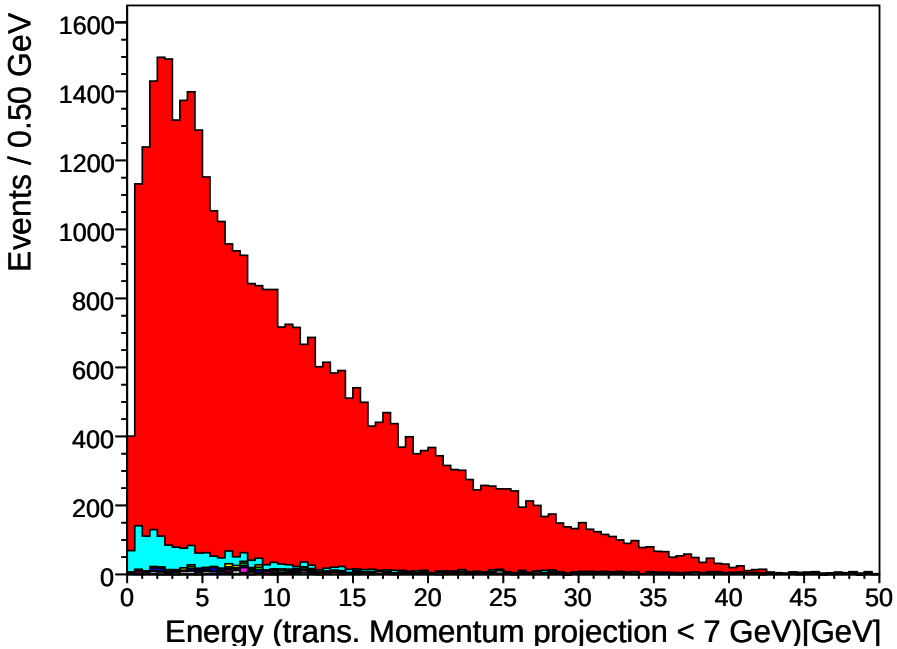

τ Polarisation

Spectrum of π:s in $\tau \rightarrow \pi^{+-}\nu_\tau$:

$$\frac{1}{\sigma}\frac{d\sigma}{dy_\pi} \sim \begin{cases} (1-P_\tau)\log\frac{P_{\tilde{\tau},max}}{P_{\tilde{\tau},min}} + 2P_\tau y_\pi\left(\frac{1}{P_{\tilde{\tau},min}} - \frac{1}{P_{\tilde{\tau},max}}\right) & \text{for } y_\pi < P_{\tilde{\tau},min} \\ (1-P_\tau)\log\frac{P_{\tilde{\tau},max}}{y_\pi} + 2P_\tau\left(1 - \frac{y_\pi}{P_{\tilde{\tau},max}}\right) & \text{for } Y_\pi > P_{\tilde{\tau},min} \end{cases}$$

Note the importance of the region with $Y_\pi < P_{\tilde{\tau},min}$!

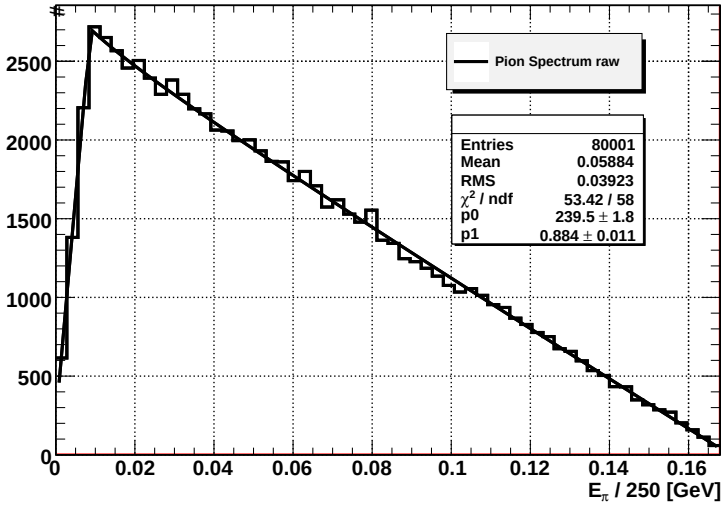

τ Polarisation : Correct expected spectrum

Correct for the spread in E_{beam}:

- Plot spectrum (at generator level), with and without beam-strahlung.
- Do this for P_τ = +1 or -1.
- Estimate correction function.
- Fit - find P_τ - re-iterate.

τ Polarisation : Correct expected spectrum

Correct for the spread in E_{beam}:

- Plot spectrum (at generator level), with and without beam-strahlung.
- Do this for P_τ = +1 or -1.
- Estimate correction function.
- Fit - find P_τ - re-iterate.

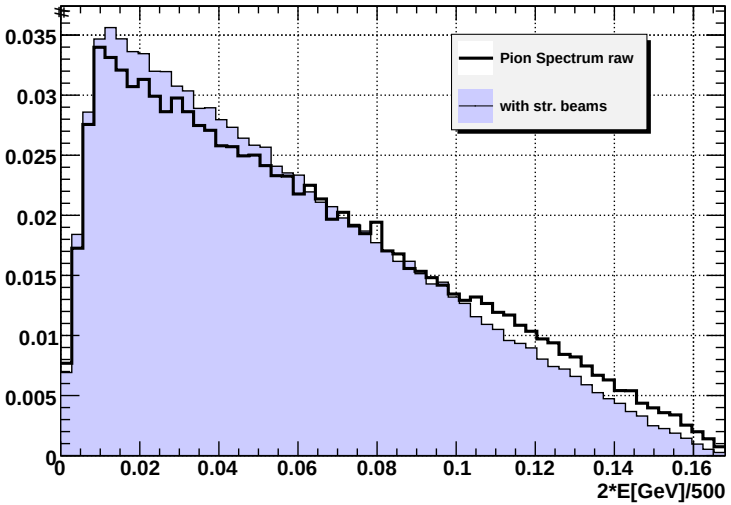

τ Polarisation : Correct expected spectrum

Correct for the spread in E_{beam}:

- Plot spectrum (at generator level), with and without beam-strahlung.
- Do this for P_τ = +1 or -1.
- Estimate correction function.
- Fit - find P_τ - re-iterate.

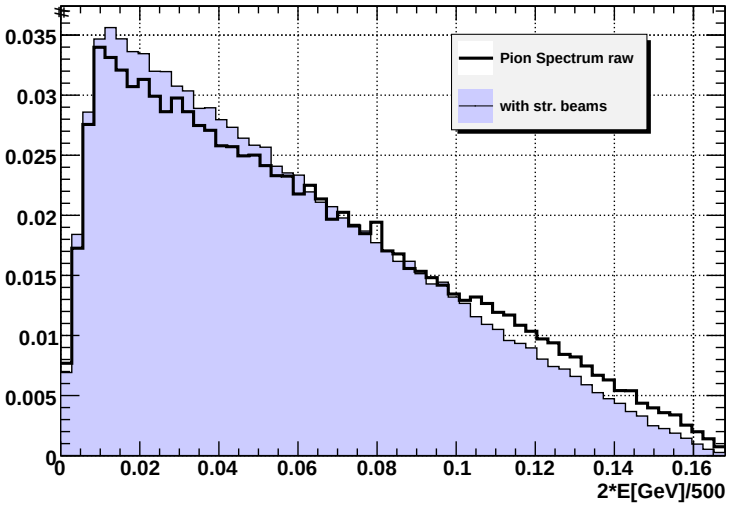

τ Polarisation : Correct expected spectrum

Correct for the spread in E_{beam}:

- Plot spectrum (at generator level), with and without beam-strahlung.
- Do this for P_τ = +1 or -1.
- Estimate correction function.
- Fit - find P_τ - re-iterate.

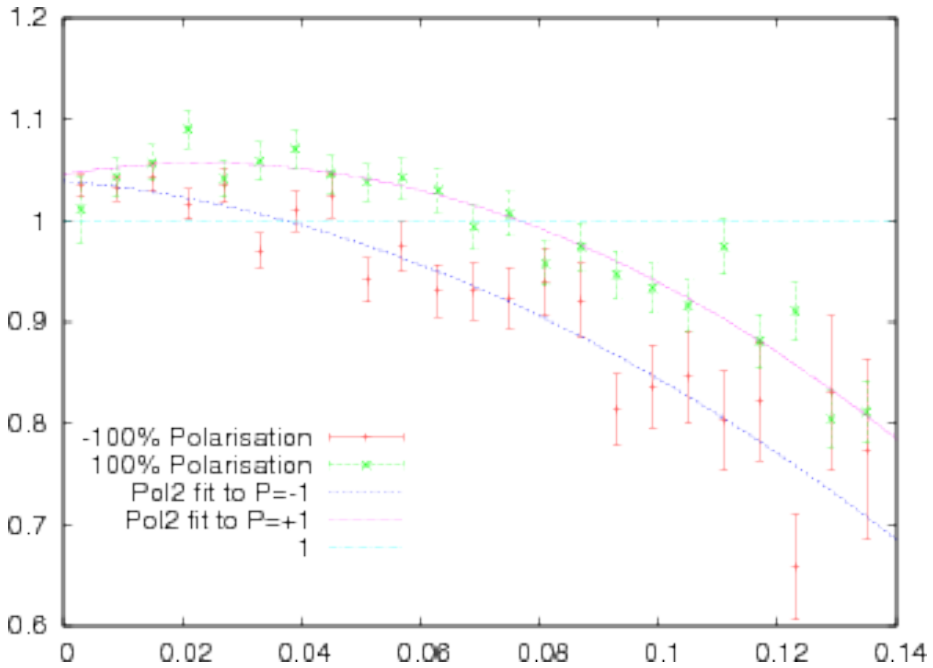

τ Polarisation : Correct expected spectrum

Correct for the spread in E_{beam}:

- Plot spectrum (at generator level), with and without beam-strahlung.
- Do this for P_τ = +1 or -1.
- Estimate correction function.
- Fit - find P_τ - re-iterate.

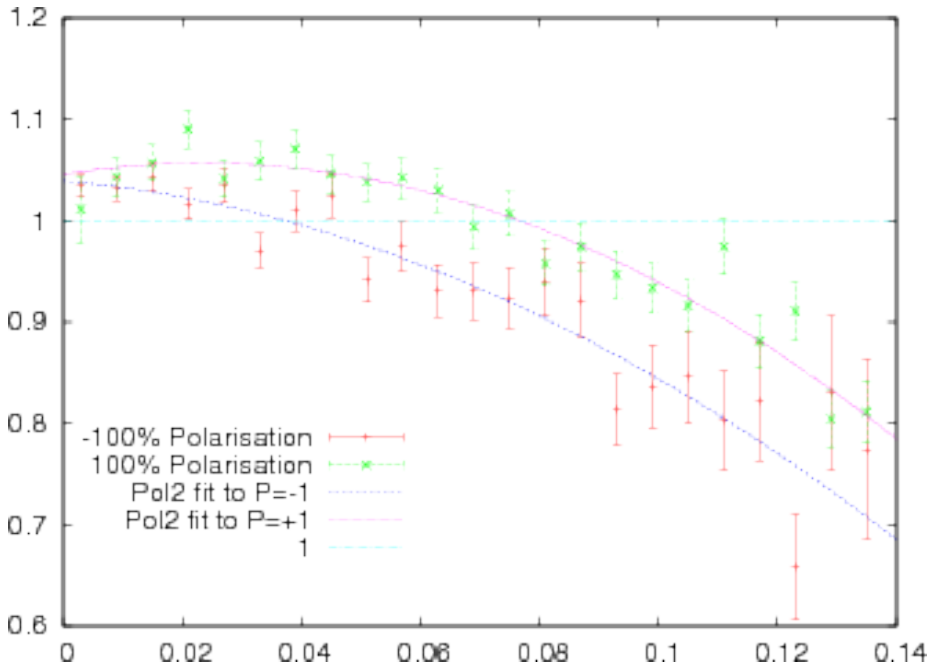

τ Polarisation: Extract signal

Extract the $\tau \rightarrow \pi^{+-}\nu_\tau$ signal. Take care to not distort the spectrum.

- Visible Energy $< 60\mathrm{GeV}$
- $|\cos\theta|$ of both jets < 0.9.
- $\cos\theta_{jet-jet} < 0.2$
- Final spectrum.

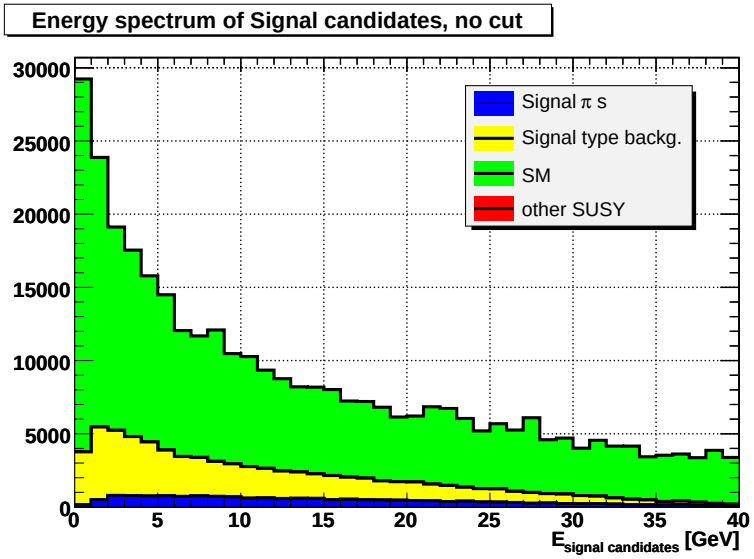

τ Polarisation: Extract signal

Extract the $\tau \rightarrow \pi^{+-}\nu_\tau$ signal. Take care to not distort the spectrum.

- Visible Energy $< 60\mathrm{GeV}$
- $|\cos\theta|$ of both jets < 0.9.
- $\cos\theta_{jet-jet} < 0.2$
- Final spectrum.

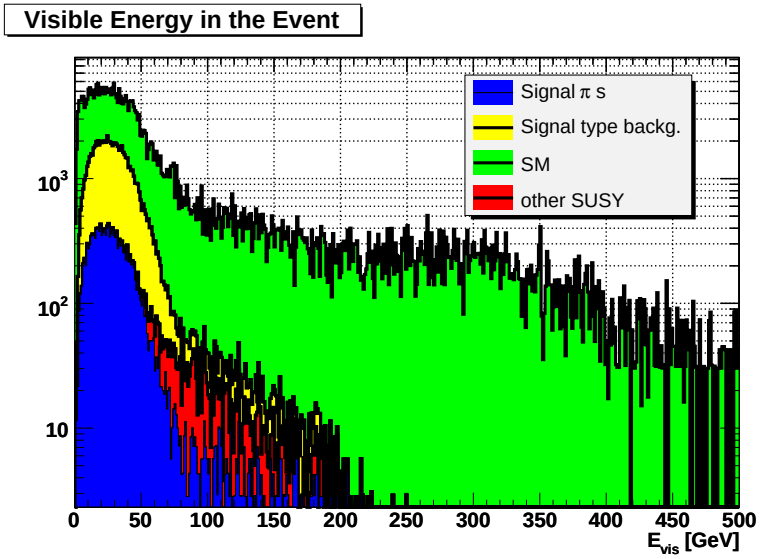

τ Polarisation: Extract signal

Extract the $\tau \rightarrow \pi^{+-}\nu_\tau$ signal. Take care to not distort the spectrum.

- Visible Energy $< 60\mathrm{GeV}$
- $|\cos\theta|$ of both jets < 0.9.
- $\cos\theta_{jet-jet} < 0.2$
- Final spectrum.

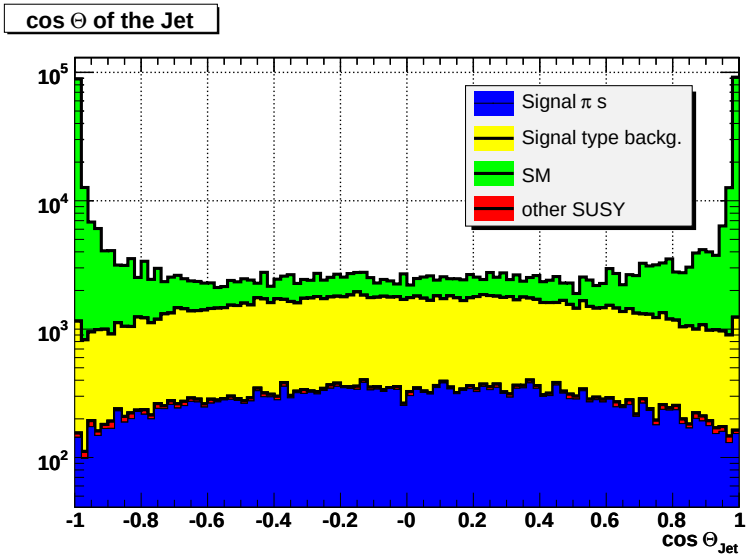

τ Polarisation: Extract signal

Extract the $\tau \rightarrow \pi^{+-}\nu_\tau$ signal. Take care to not distort the spectrum.

- Visible Energy $< 60\mathrm{GeV}$
- $|\cos\theta|$ of both jets < 0.9.
- $\cos\theta_{jet-jet} < 0.2$
- Final spectrum.

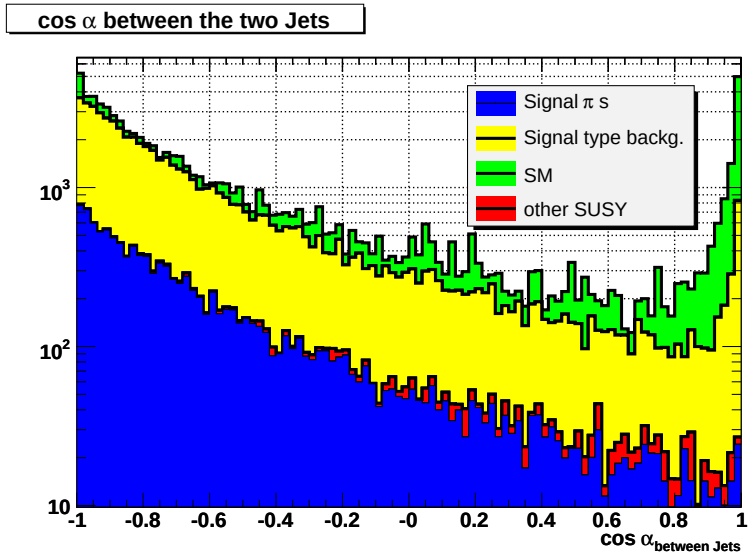

τ Polarisation: Extract signal

Extract the $\tau \rightarrow \pi^{+-}\nu_\tau$ signal. Take care to not distort the spectrum.

- Visible Energy $< 60\mathrm{GeV}$
- $|\cos\theta|$ of both jets < 0.9.
- $\cos\theta_{jet-jet} < 0.2$
- Final spectrum.

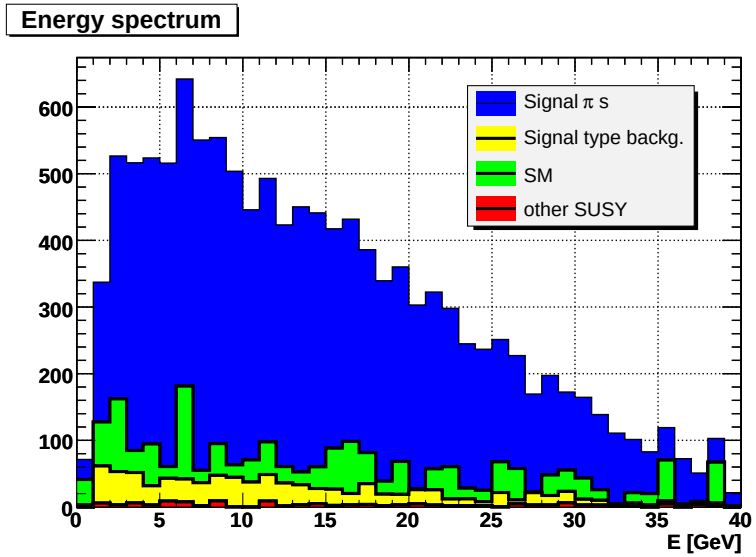

τ Polarisation : background and signal fit

(Present) method to extract the polarisation:

- Fit background.
- Invert cuts, and scale the fitted background.
- Check if shape is OK.
- If yes, fit background to inverted cuts, scale down to agree in non-signal region.
- Subtract this background estimate.
- Apply efficiency correction.
- Fit.

$P_\tau = (93 \pm 9)\ \%$

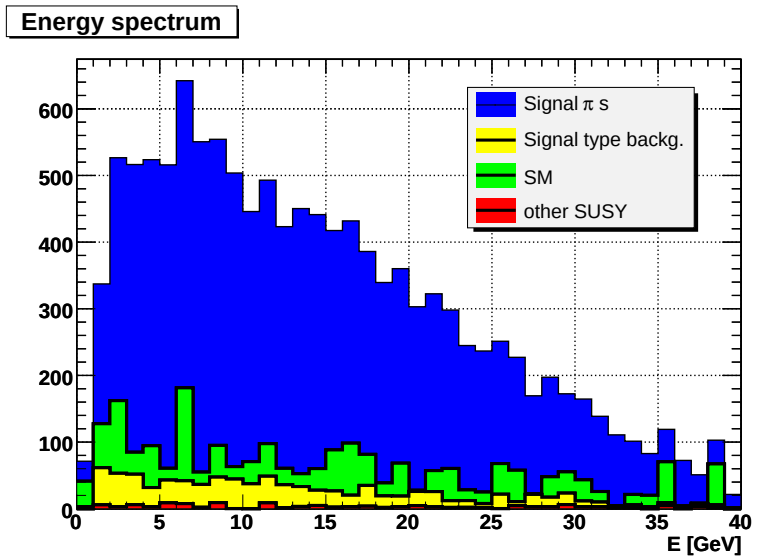

τ Polarisation : background and signal fit

(Present) method to extract the polarisation:

- Fit background.
- Invert cuts, and scale the fitted background.
- Check if shape is OK.
- If yes, fit background to inverted cuts, scale down to agree in non-signal region.
- Subtract this background estimate.
- Apply efficiency correction.
- Fit.

$P_\tau = (93 \pm 9)\ \%$

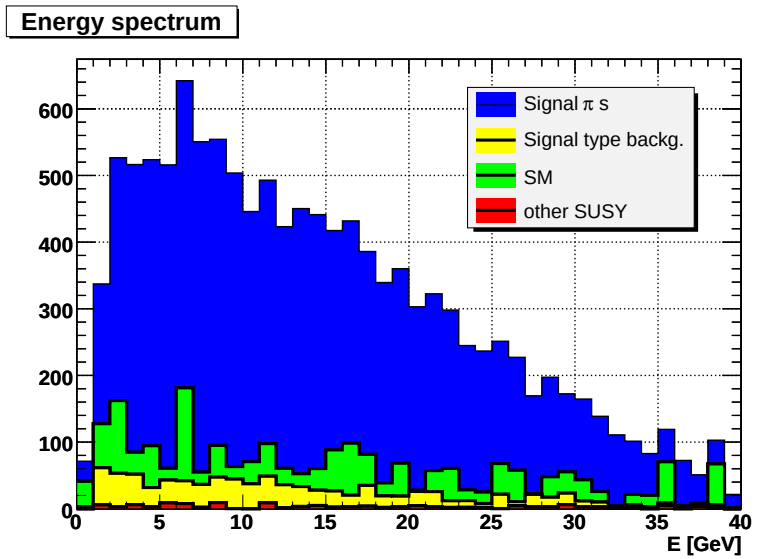

τ Polarisation : background and signal fit

(Present) method to extract the polarisation:

- Fit background.
- Invert cuts, and scale the fitted background.
- Check if shape is OK.
- If yes, fit background to inverted cuts, scale down to agree in non-signal region.
- Subtract this background estimate.
- Apply efficiency correction.
- Fit.

$P_\tau = (93 \pm 9)\ \%$

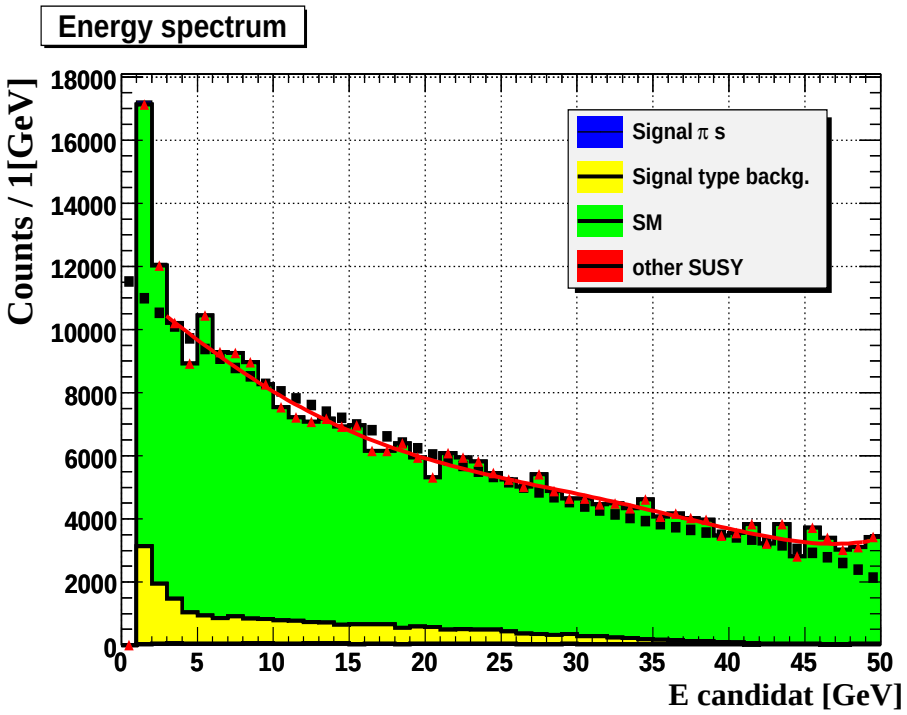

τ Polarisation : background and signal fit

(Present) method to extract the polarisation:

- Fit background.
- Invert cuts, and scale the fitted background.
- Check if shape is OK.
- If yes, fit background to inverted cuts, scale down to agree in non-signal region.
- Subtract this background estimate.
- Apply efficiency correction.
- Fit.

$P_\tau = (93 \pm 9)\ \%$

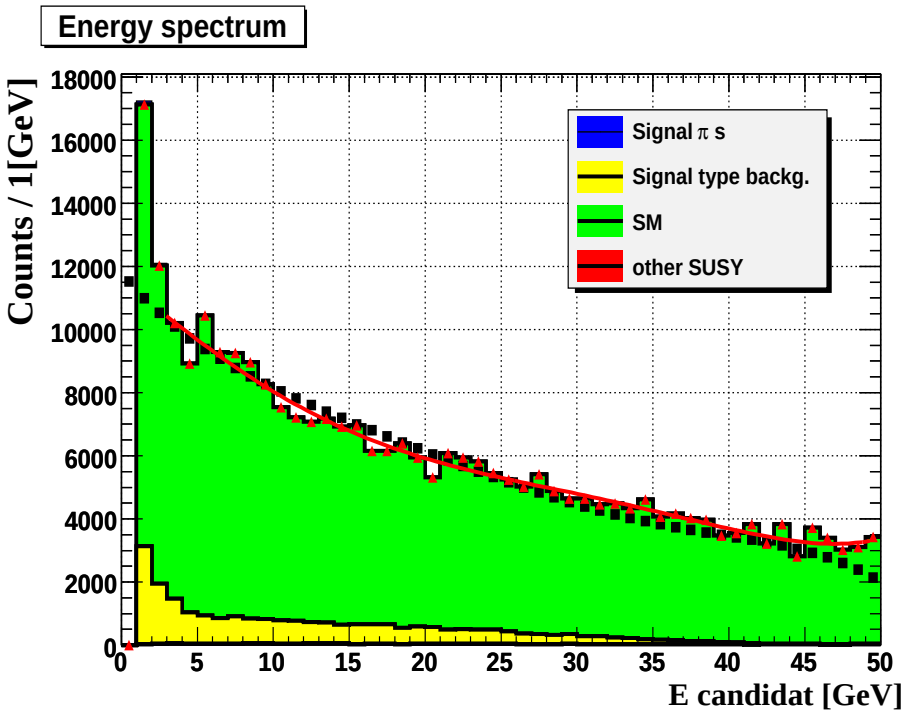

τ Polarisation : background and signal fit

(Present) method to extract the polarisation:

- Fit background.
- Invert cuts, and scale the fitted background.
- Check if shape is OK.
- If yes, fit background to inverted cuts, scale down to agree in non-signal region.
- Subtract this background estimate.
- Apply efficiency correction.
- Fit.

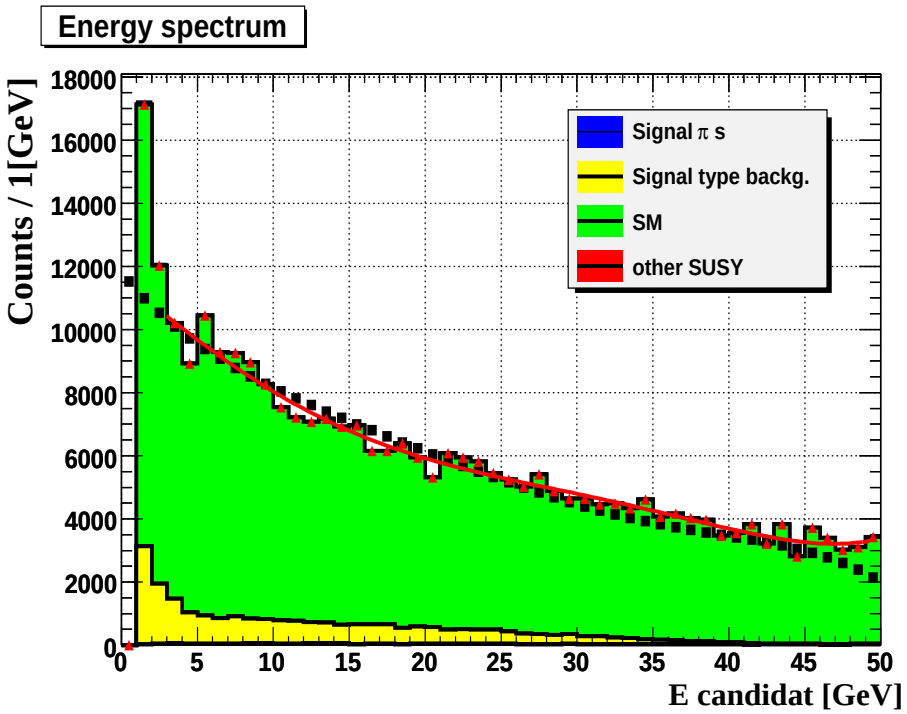

$P_\tau = (93 \pm 9)\ \%$

τ Polarisation : background and signal fit

(Present) method to extract the polarisation:

- Fit background.
- Invert cuts, and scale the fitted background.
- Check if shape is OK.
- If yes, fit background to inverted cuts, scale down to agree in non-signal region.
- Subtract this background estimate.
- Apply efficiency correction.
- Fit.

$P_\tau = (93 \pm 9)\ \%$

τ Polarisation : background and signal fit

(Present) method to extract the polarisation:

- Fit background.
- Invert cuts, and scale the fitted background.
- Check if shape is OK.
- If yes, fit background to inverted cuts, scale down to agree in non-signal region.
- Subtract this background estimate.
- Apply efficiency correction.
- Fit.

$P_\tau = (93 \pm 9)\ \%$

τ Polarisation : background and signal fit

(Present) method to extract the polarisation:

- Fit background.
- Invert cuts, and scale the fitted background.
- Check if shape is OK.
- If yes, fit background to inverted cuts, scale down to agree in non-signal region.
- Subtract this background estimate.
- Apply efficiency correction.
- Fit.

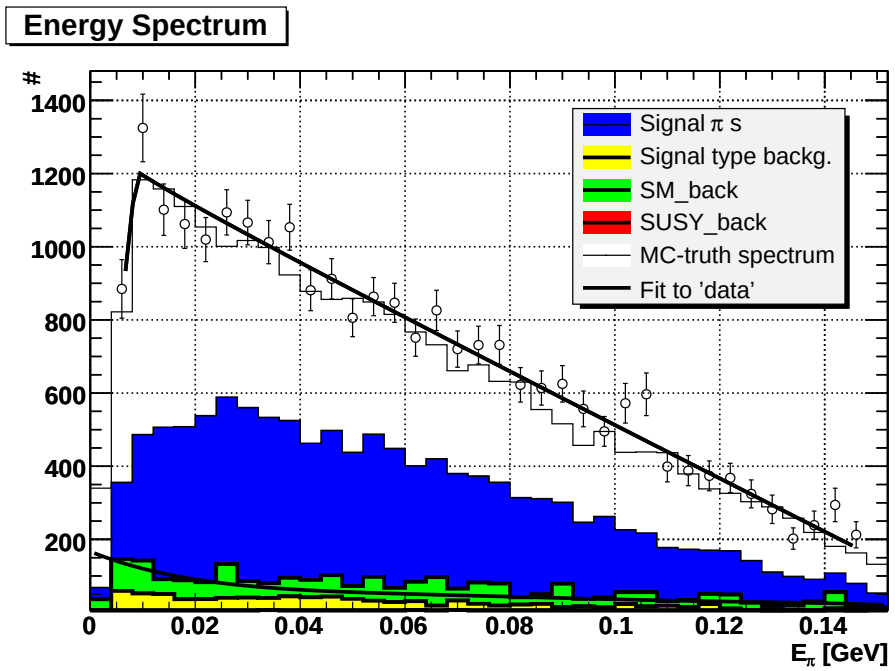

$P_\tau = (93 \pm 9)\ \%$

τ Polarisation : background and signal fit

(Present) method to extract the polarisation:

- Fit background.
- Invert cuts, and scale the fitted background.
- Check if shape is OK.
- If yes, fit background to inverted cuts, scale down to agree in non-signal region.
- Subtract this background estimate.
- Apply efficiency correction.
- Fit.

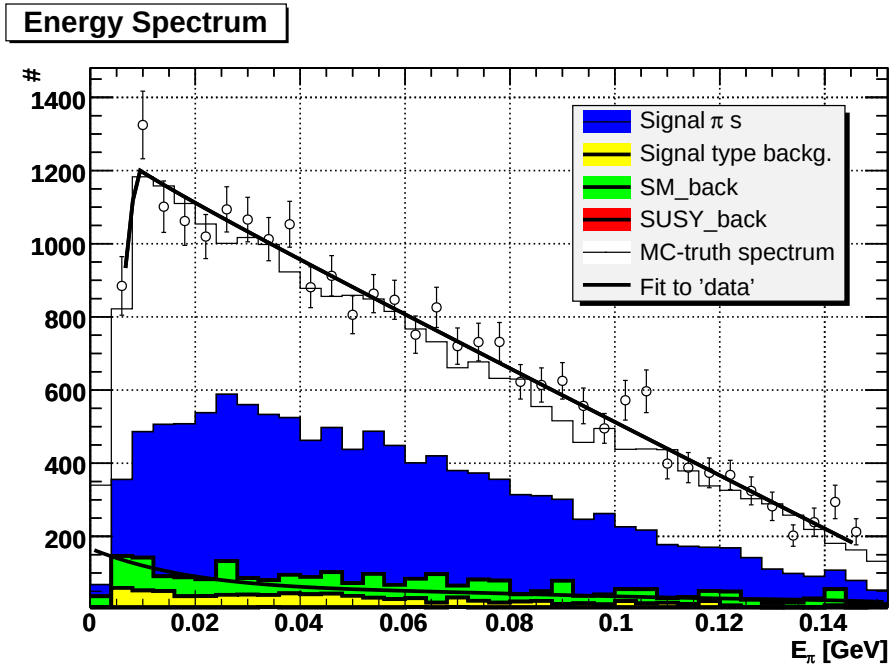

$P_\tau = (93 \pm 9)\ \%$

Summary and outlook

Full simulation of some channels in SPS1a' in the LDC' detector was presented

- A finalised analysis of μ-channels.
- For $\mathrm{e^+e^-} \rightarrow \tilde{\mu}_\mathrm{L}\tilde{\mu}_\mathrm{L}$, we find: $\Delta(M_{\tilde{\chi}_1^0}) = 920\mathrm{MeV}/c^2$
  $\Delta(M_{\tilde{\mu}_\mathrm{L}}) = 100\mathrm{MeV}/c^2$
  $\Delta(\sigma(\mathrm{e^+e^-} \rightarrow \tilde{\mu}_\mathrm{L}\tilde{\mu}_\mathrm{L}))$ = 1.35 fb.
- For $\tilde{\chi}_1^0\tilde{\chi}_2^0 \rightarrow \mu\tilde{\mu}_\mathrm{R}\tilde{\chi}_1^0 \rightarrow \mu\mu\tilde{\chi}_1^0\tilde{\chi}_1^0$, we find $\Delta(M_{\tilde{\chi}_2^0}) = 1.38\mathrm{GeV}/c^2$, comparable to what the threshold scan would give.
- A progress report on $\tilde{\tau}$ production was given. .
- A very preliminary result: $\Delta(P_\tau) = 9$ %.

Outlook:

- Complete $\tilde{\tau}$ analysis, include $\gamma\gamma$ background, and use ILD.

Summary and outlook

Full simulation of some channels in SPS1a' in the LDC' detector was presented

- A finalised analysis of μ-channels.
- For $\mathrm{e^+e^-} \rightarrow \tilde{\mu}_\mathrm{L}\tilde{\mu}_\mathrm{L}$, we find: $\Delta(M_{\tilde{\chi}_1^0}) = 920\mathrm{MeV}/c^2$
  $\Delta(M_{\tilde{\mu}_\mathrm{L}}) = 100\mathrm{MeV}/c^2$
  $\Delta(\sigma(\mathrm{e^+e^-} \rightarrow \tilde{\mu}_\mathrm{L}\tilde{\mu}_\mathrm{L}))$ = 1.35 fb.
- For $\tilde{\chi}_1^0\tilde{\chi}_2^0 \rightarrow \mu\tilde{\mu}_\mathrm{R}\tilde{\chi}_1^0 \rightarrow \mu\mu\tilde{\chi}_1^0\tilde{\chi}_1^0$, we find $\Delta(M_{\tilde{\chi}_2^0}) = 1.38\mathrm{GeV}/c^2$, comparable to what the threshold scan would give.
- A progress report on $\tilde{\tau}$ production was given. .
- A very preliminary result: $\Delta(P_\tau) = 9$ %.

Outlook:

- Complete $\tilde{\tau}$ analysis, include $\gamma\gamma$ background, and use ILD.

Summary and outlook

Full simulation of some channels in SPS1a' in the LDC' detector was presented

- A finalised analysis of μ-channels.
- For $\mathrm{e^+e^-} \rightarrow \tilde{\mu}_\mathrm{L}\tilde{\mu}_\mathrm{L}$, we find: $\Delta(M_{\tilde{\chi}_1^0}) = 920\mathrm{MeV}/c^2$
  $\Delta(M_{\tilde{\mu}_\mathrm{L}}) = 100\mathrm{MeV}/c^2$
  $\Delta(\sigma(\mathrm{e^+e^-} \rightarrow \tilde{\mu}_\mathrm{L}\tilde{\mu}_\mathrm{L}))$ = 1.35 fb.
- For $\tilde{\chi}_1^0\tilde{\chi}_2^0 \rightarrow \mu\tilde{\mu}_\mathrm{R}\tilde{\chi}_1^0 \rightarrow \mu\mu\tilde{\chi}_1^0\tilde{\chi}_1^0$, we find $\Delta(M_{\tilde{\chi}_2^0}) = 1.38\mathrm{GeV}/c^2$, comparable to what the threshold scan would give.
- A progress report on $\tilde{\tau}$ production was given. .
- A very preliminary result: $\Delta(P_\tau) = 9$ %.

Outlook:

- Complete $\tilde{\tau}$ analysis, include $\gamma\gamma$ background, and use ILD.

Summary and outlook

Full simulation of some channels in SPS1a' in the LDC' detector was presented

- A finalised analysis of μ-channels.
- For $\mathrm{e^+e^-} \rightarrow \tilde{\mu}_\mathrm{L}\tilde{\mu}_\mathrm{L}$, we find: $\Delta(M_{\tilde{\chi}_1^0}) = 920\mathrm{MeV}/c^2$
  $\Delta(M_{\tilde{\mu}_\mathrm{L}}) = 100\mathrm{MeV}/c^2$
  $\Delta(\sigma(\mathrm{e^+e^-} \rightarrow \tilde{\mu}_\mathrm{L}\tilde{\mu}_\mathrm{L}))$ = 1.35 fb.
- For $\tilde{\chi}_1^0\tilde{\chi}_2^0 \rightarrow \mu\tilde{\mu}_\mathrm{R}\tilde{\chi}_1^0 \rightarrow \mu\mu\tilde{\chi}_1^0\tilde{\chi}_1^0$, we find $\Delta(M_{\tilde{\chi}_2^0}) = 1.38\mathrm{GeV}/c^2$, comparable to what the threshold scan would give.
- A progress report on $\tilde{\tau}$ production was given. .
- A very preliminary result: $\Delta(P_\tau) = 9$ %.

Outlook:

- Complete $\tilde{\tau}$ analysis, include $\gamma\gamma$ background, and use ILD.

Summary and outlook

Full simulation of some channels in SPS1a' in the LDC' detector was presented

- A finalised analysis of μ-channels.
- For $\mathrm{e^+e^-} \rightarrow \tilde{\mu}_\mathrm{L}\tilde{\mu}_\mathrm{L}$, we find: $\Delta(M_{\tilde{\chi}_1^0}) = 920\mathrm{MeV}/c^2$
  $\Delta(M_{\tilde{\mu}_\mathrm{L}}) = 100\mathrm{MeV}/c^2$
  $\Delta(\sigma(\mathrm{e^+e^-} \rightarrow \tilde{\mu}_\mathrm{L}\tilde{\mu}_\mathrm{L}))$ = 1.35 fb.
- For $\tilde{\chi}_1^0\tilde{\chi}_2^0 \rightarrow \mu\tilde{\mu}_\mathrm{R}\tilde{\chi}_1^0 \rightarrow \mu\mu\tilde{\chi}_1^0\tilde{\chi}_1^0$, we find $\Delta(M_{\tilde{\chi}_2^0}) = 1.38\mathrm{GeV}/c^2$, comparable to what the threshold scan would give.
- A progress report on $\tilde{\tau}$ production was given. .
- A very preliminary result: $\Delta(P_\tau) = 9$ %.

Outlook:

- Complete $\tilde{\tau}$ analysis, include $\gamma\gamma$ background, and use ILD.

Summary and outlook

Full simulation of some channels in SPS1a' in the LDC' detector was presented

- A finalised analysis of μ-channels.
- For $\mathrm{e^+e^-} \rightarrow \tilde{\mu}_\mathrm{L}\tilde{\mu}_\mathrm{L}$, we find: $\Delta(M_{\tilde{\chi}_1^0}) = 920\mathrm{MeV}/c^2$
  $\Delta(M_{\tilde{\mu}_\mathrm{L}}) = 100\mathrm{MeV}/c^2$
  $\Delta(\sigma(\mathrm{e^+e^-} \rightarrow \tilde{\mu}_\mathrm{L}\tilde{\mu}_\mathrm{L}))$ = 1.35 fb.
- For $\tilde{\chi}_1^0\tilde{\chi}_2^0 \rightarrow \mu\tilde{\mu}_\mathrm{R}\tilde{\chi}_1^0 \rightarrow \mu\mu\tilde{\chi}_1^0\tilde{\chi}_1^0$, we find $\Delta(M_{\tilde{\chi}_2^0}) = 1.38\mathrm{GeV}/c^2$, comparable to what the threshold scan would give.
- A progress report on $\tilde{\tau}$ production was given. .
- A very preliminary result: $\Delta(P_\tau) = 9$ %.

Outlook:

- Complete $\tilde{\tau}$ analysis, include $\gamma\gamma$ background, and use ILD.